**João Nuno
Pinheiro Maciel**

**Combinação do código de Alamouti e OFDM para
a Integração dos Futuros Sistemas MIMO de radar
e comunicações**

**The combination of Alamouti Coding with OFDM
for the Integration of the future MIMO Radar and
Communication Systems**

**João Nuno
Pinheiro Maciel**

**Combinação do código de Alamouti e OFDM para
a Integração dos Futuros Sistemas MIMO de radar
e comunicações**

**The combination of Alamouti Coding with OFDM
for the Integration of the future MIMO Radar and
Communication Systems**

o júri / the jury

presidente / president

Professor Doutor João Nuno Pimentel da Silva Matos
Professor Associado da Universidade de Aveiro

vogais / examiners committee

Professor Doutor Rui Miguel Henriques Dias Morgado Dinis
Professor Associado com Agregação da Universidade Nova de Lisboa

Professor Doutor Adão Paulo Soares da Silva
Professor Auxiliar da Universidade de Aveiro

**agradecimentos /
acknowledgements**

Palavras-Chave   IoT, OFDM, MIMO, Radar, RadCom.

Resumo   A necessidade por largura de banda de radiofrequência, está a aumentar com o crescente número de utilizadores e aplicações. Os sistemas de radar e comunicações, são dois dos principais intervenientes nesta matéria e fundamentais para fazer do paradigma da IoT uma realidade. A separação dos sistemas de radar e comunicação, é um desperdício de recurso sendo a interferência entre os dois sistemas inevitável. Por outro lado, a integração em um único hardware, permite o paradigma de dispositivos de funcionalidade dupla com capacidades de comunicação e radar, fundamentais para lidar com os desafios da futura IoT.

Nesta dissertação, a integração de sistemas de radar e comunicação é realizada usando OFDM, como forma de onda comum. O uso da codificação de Alamouti permite tanto a obtenção de diversidade espacial, para a funcionalidade de comunicação, como a ortogonalidade do sinal de transmissão necessária para melhorar a resolução da functionalidade do radar. A avaliação de tais métodos como uma maneira de alcançar a integração de radar e comunicação foi alcançada através do desenvolvimento de uma plataforma de simulação. Primeiro, apenas com a funcionalidade radar, para configurações SISO e MIMO. Por fim, com as funcionalidades de radar e comunicação. O sistema proposto apresenta bom desempenho, baixa complexidade e por isso interessante para aplicações práticas.

Abstract   The demand for radio-frequency bandwidth is rising, with the growing number of users and applications. The radar and communication systems are two of main players in this regard and are central to make the IoT paradigm a reality. The separation of the radar and communication system is a waste of resources and the interference between the two systems is inevitable. On the other hand, their integration on a single hardware, enables the paradigm of dual functionality devices with communication and radar sensing capabilities fundamental to cope with the challenges of future IoT.

In this dissertation, the integration of radar and communication systems is accomplished by using OFDM as a common waveform and the use of Alamouti coding enables both the achievement of spatial diversity, for the communication functionality, and of transmit signal orthogonality required to improve resolution, for the radar functionality. The evaluation of such methods as a way to achieve radar and communication integration was accomplished by developing a simulation platform, first only with the radar functionality, for SISO and MIMO configurations, and then with both radar and communication functionalities. The RadCom system developed present good performance, low complexity and so it is interesting for practical applications.

Contents

List of Figures

List of Tables

Acronyms

1G	1st Generation
2D	Two-Dimensional
2G	2nd Generation
3G	3rd Generation
4G	4th Generation
5G	5th Generation
AWGN	Additive White Gaussian Noise
BER	Bit Error Rate
BPSK	Binary Phase Shift Keying
CDMA	Code Division Multiple Access
CP	Cyclic Prefix
CW	Continuous Wave
D-AMPS	Digital Advanced Mobile Phone System
DAB	Digital Audio Broadcasting
DVB	Digital Video Broadcasting
EGC	Equal Gain Combining
FBMC	Filter Bank Multicarrier
FFT	Fast Fourier Transform
FM	Frequency Modulation
FMCW	Frequency-Modulated Continuous Wave
GFDM	Generalized Frequency Division Multiplexing
GPS	Global Positioning System
GSM	Global System for Mobile Communications
ICI	Inter Carrier Interference
IEEE	Institute of Electrical and Electronic Engineering

IFFT	Inverse Fast Fourier Transform
IoT	Internet of Things
ISI	Intersymbol Interference
ISM	The Industrial, Scientific and Medical
ITS	Intelligent Transportation Systems
ITU	International Telecommunications Union
LTE	Long-Term Evolution
MIMO	Multiple-Input Multiple-Output
MISO	Multiple-Input Single-Output
mmWave	Millimeter Wave
MRC	Maximum Ratio Combining
NASA	National Aeronautics and Space Administration
OFDM	Orthogonal Frequency Division Multiplexing
OFDMA	Orthogonal Frequency Division Multiple Access
PSK	Phase Shift Keying
QAM	Quadrature Amplitude Modulation
Radar	Radio Detection and Ranging
RadCom	Radar and Communication
RCS	Radar Cross Section
RF	Radio Frequency
SC	Selection Combining
SC-FDMA	Single Carrier Frequency Division Multiple Access
SE	Spectral Efficiency
SFBC	Space-Frequency Block Code
SFCW	Stepped-Frequency Continuous Wave
SISO	Single-Input Multiple-Output
SISO	Single-Input Single-Output
SNR	Signal-to-Noise Ratio
STBC	Space-Time Block Code
STTC	Space-Time Trellis Code

TDMA	Time Division Multiple Access
UFMC	Universal Filtered Multicarrier
ULVA	Uniform Linear Virtual Array
V2V	Vehicle-to-Vehicle
WCDMA	Wideband Code Division Multiple Access
WiMAX	Worldwide Interoperability for Microwave Access
WSN	Wireless Sensor Networks

x

Chapter 1

Introduction

This Chapter introduces the background of the radars and communications systems. The first section discusses the evolution of the communication systems and the second one focus on the joint radar and communication systems, followed by some applications, then the objectives and motivation and the structure of this work is presented.

1.1   Communication Systems

The first generation (1G) introduced in 1980s, provided a basic voice service using analog transmission. The rise of second generation (2G), third generation (3G) and fourth generation (4G) and the impact of these systems worldwide, led us to talk today about the fifth generation (5G). The success of these systems is due to the fact that they offers mobility, portability and ease connection that allows to free the user from a physical connection to a network. Such characteristics that made it a powerful tool also made it indispensable to the people's life.

Starting with the first generation, the technology was supported by different systems in different countries, at that time: Nippon Telephone and Telegraph (NTT) in, Japan; Nordic Mobile Telephone (NMT) and Total Access Communication System (TACS) in Europe; Advance mobile phone system (AMPS) in USA. All the systems offered roaming capability, but the cellular networks were unable to interoperate between countries [1]. The need for such systems to be compatible and interoperable with each other and to go along with the growing market of mobile communication, a strait policy of technology standardization become more serious.

The second generation, brought the digital technology. This generation emerged in 1990's and was supported by digital multiple access technology, like time division multiple access (TDMA) and code division multiple access (CDMA) [2]. The upgrade from analog to digital, brought considerably higher efficiency at the spectrum level and also enabled the mobile data services, beginning with the short message service (SMS). The systems deployed for this generation were: Global System for Mobile Communications (GSM) in the European countries; Digital Advanced Mobile Phone System (D-AMPS) IS-54 in the USA; Japanese Digital Cellular (JDC) in Japan and Code Division Multiple Access (CDMA) by Qualcomm, USA [3].
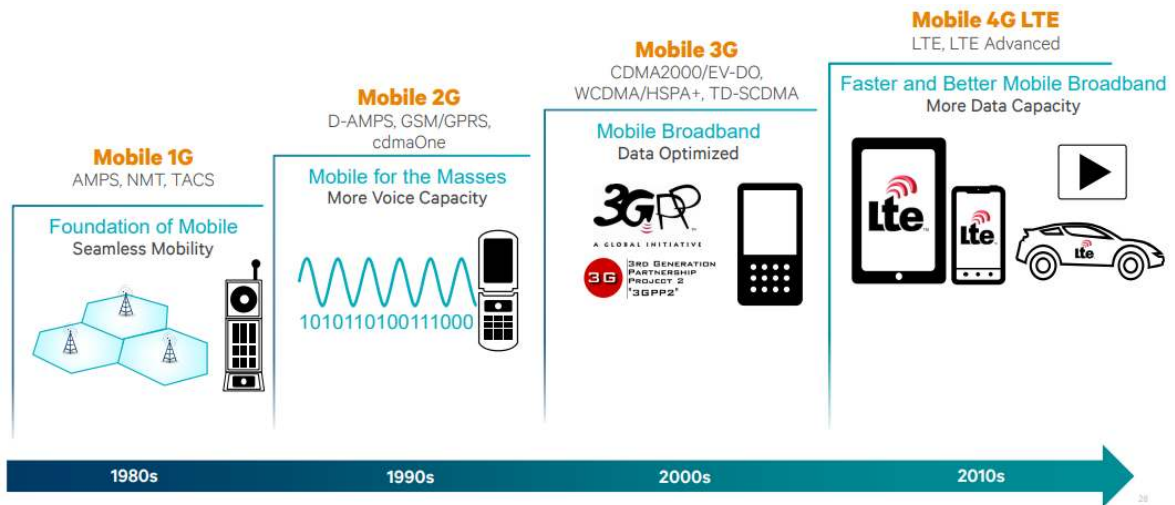
Figure 1.1: Evolution of the Mobile Communication System [4].

The third generation technology, was based on a plan denominated the International Mobile Telecommunications-2000 (IMT-2000), created by the International Telecommunication Union (ITU) to implement the wireless communication standards for all countries [1]. This technology had as main objective to provide higher data-rate services [5]. The services included wide area wireless voice, telephony, video calls, and broadband wireless data, mobile television, global positioning system (GPS) and video conferencing, all in a mobile environment [1]. One of the aspects of the 3G was the choice of CDMA as the preferred access technique for the majority of 3G systems [6]. Two concepts were created based on CDMA schemes the Wideband Code Division Multiple Access (WCDMA) and CDMA 2000 [3].

The Fourth Generation provides access to a wide range of telecommunication services, including advanced mobile services, supported by mobile and fixed networks, along with a support for low to high mobility applications and wide range of data rates [1]. The standard technologies considered for the 4G include the Long Term Evolution (LTE), Ultra Mobile Broadband and World wide Interoperability for Microwave Access (WiMAX) [7]. The 4G was marked by the LTE interface that employs two main technologies: the Orthogonal Frequency Division Multiple Access (OFDMA) for downlink and Single Carrier Frequency Division Multiple Access (SC-FDMA) for uplink. The continuous development of LTE led to the appearance of LTE-Advanced. The Figure 1.1 illustrate the evolution of the mobile communications.

The fifth generation network technology will open a new era in mobile communication technology. Unlike previous systems, which focused on providing voice and data services, 5G focuses on users and their needs. It seems that 2020 will be the year that Fifth Generation technology will arrive in the global telecommunication market [1]. 5G wireless networks will support up to a 1000-fold increase in capacity compared to existing networks. It is anticipated to connect at least 100 billion devices worldwide with approximately 7.6 billion mobile subscribers due to the tremendous popularity of smart-phones, electronic tablets, sensors, and so on. It is expected an individual user experience up to 10 Gb/s [8]. The expected subscription

2

growth, by mobile technology, is illustrated in Figure 1.2. Along with the dramatic traffic explosion and device proliferation, 5G also has to integrate human-to-machine and machine-to-machine communications in order to facilitate more flexible networked social information sharing aiming for one million connections per square kilometer [9].
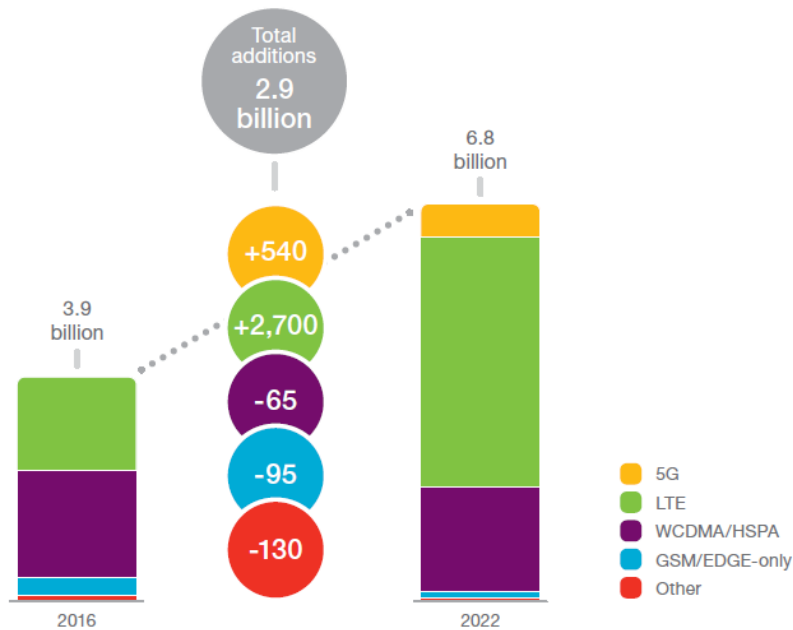
Figure 1.2: Mobile smartphone subscriptions by technology [8].

To achieve all the service requirements 5G face some design challenges. The Figure 1.3 summarize the parameters and make a comparison between 4G e 5G. Some of the requirements are mentioned below [1],[10]:

- **Reduced Latency:** is expected that 5G will be able to support a roundtrip latency of about 1 ms. Reducing latency leads to achieving high data rates and faster response times but could also introduce new use cases such as remote control of machines.

- **Higher User Mobility:** is expected that the existing mobile services continue with the natural evolution but it is also expected that new ones, such as autonomous driving, vehicle-to-vehicle communications, traffic safety and other services will emerge. Therefore, there is a pressing need for higher user mobility.

- **Low Battery Consumption:** the reduction of energy consumption in devices play a key role. Some of the expected technologies in 5G will require an uninterrupted operation of devices. For example, remote health services, automotive and virtual reality.

- **Higher Data Rates:** Services as realtime gaming, augmented reality, remote controlled vehicles, cloud services and machine to machine communications will be common among users. In order to provide a good service a high data rate service is necessary.
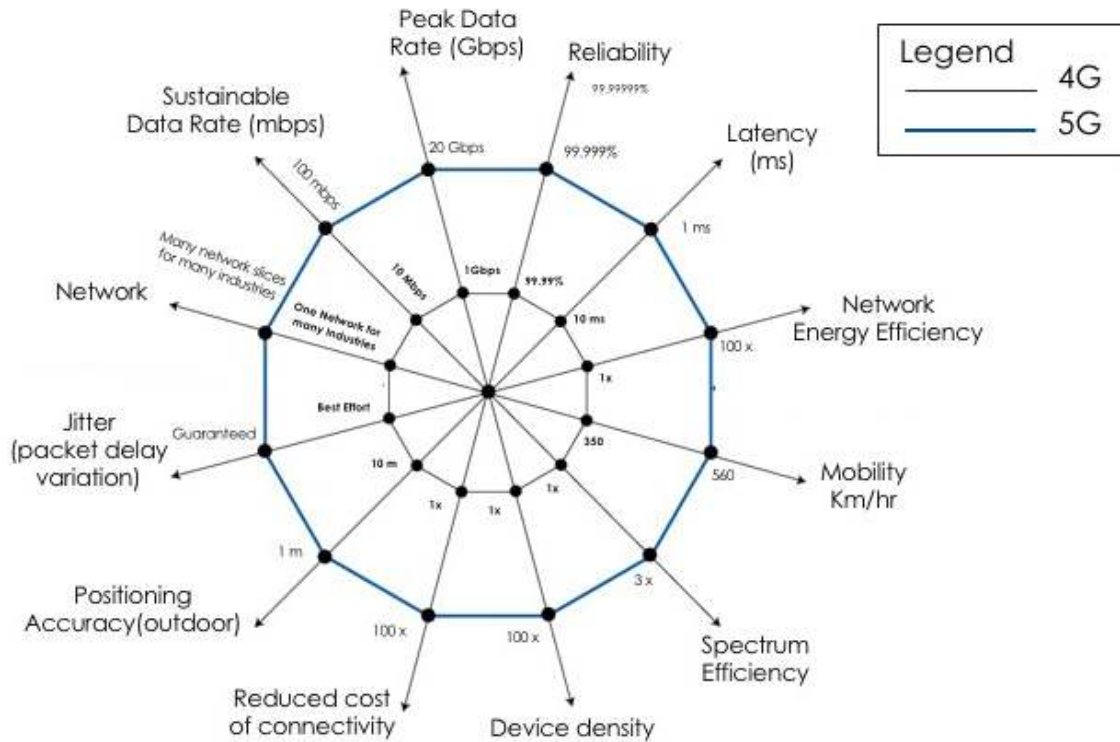
Figure 1.3: 5G requirements [11].

Some of this requirements can be achieved through some potential technologies [10]. The multiple-input multiple-output (MIMO) technique employs multiple antennas at the transmitter and receiver, serving multiple users using the same time frequency resources. Such technique is used to increase the spectral efficiency (SE) of a wireless link. Massive MIMO extends the MIMO concept by dramatically increasing the number of antennas employed, serving tens of users simultaneously and increasing the spectral efficiency 5 times to 10 [12]. The use of frequencies above 10 GHz is being considered for 5G. Frequencies around 30 GHz until 300 GHz are in the millimeter wavelength band. The use of millimeter waves(mmWave) compared to lower frequencies bands results in an increased bandwidth. Extreme densification can be a solution as well to improve the area spectral efficiency [10]. These are some of the solutions under study.

A fully mobile and connected society is expected in the near future, which will be characterized by a tremendous amount of growth in connectivity, traffic volume, and a much broader range of usage scenarios [13]. The Internet of Things (IoT) will be one of the main drivers in the future development of mobile communications. The Internet of Things (IoT) initially utilized current internet infrastructure and existing technologies to transform stand-alone devices into interconnected smart objects [14]. From the point of view of a private user, the most obvious effects of the IoT introduction will be visible in both working and domestic fields [15].

4

1.2 Joint Radar and Communication Systems

The first radar was patented in 1904 by Christian Hulsmeyer. It was a pulsed radar, radiating differentiated pulses, generated by a spark gap [16]. Compared to several decades ago radar applications have spread to many new areas like automotive radars, surveillance, sensors, automation control, medical applications, imaging, remote sensing and so on [17]. Such applications were what maintained the radar technology alive.

There are radars that only listen and analyze what is around them using signals emitted by other systems, named as passive radars [18]. This radar system fits to the bistatic topology. Passive radar systems may be used for military surveillance and civil applications such as airspace surveillance and surface monitoring [19]. FM radio, cellular base stations, satellite systems, Digital Audio Broadcasting (DAB) and Digital Video Broadcasting (DVB) are communication systems that can be used as passive radar sources [19]. Some of these systems use OFDM modulated signals, in [20] the use of DVB signals as a radar system for traffic density monitoring, is studied. The Figure 1.4 shows a scenario of a bistatic system that uses a shared waveform for both the communication link and the radar.
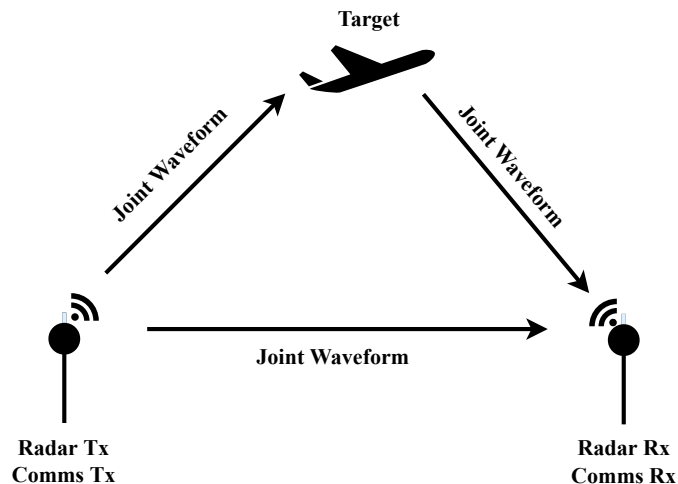
Figure 1.4: Bistatic topology.

On the other hand we have the active radars. The active radars fits in the monostatic topology and can be illustrated by the scenario presented in Figure 1.5. The system illustrated also uses a shared waveform for both the communication link and the radar system. Consider the scenario illustrated in Figure 1.6, where the radar system and the communication system are designed in isolation. The introduction of a shared waveform used for joint radar and communications will benefit both systems, since it can be the, for example, a solution for problems like spectral congestion.

Wireless communication and radar systems represent two different types of systems that utilize the radio frequency (RF) spectrum. While these systems have traditionally been designed separately from each other, they share many similar properties that can facilitate a

Target

Joint Waveform

Joint Waveform

Joint Waveform

Radar Tx
Radar Rx
Comms Tx

Comms Rx
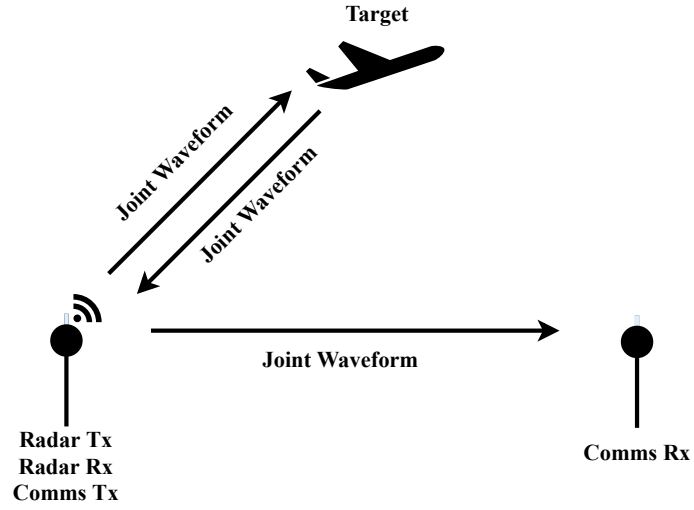
Figure 1.5: Monostatic topology.

Target

External
Interference

Radar Waveform

Radar Waveform

Radar Waveform

Radar Waveform

Comm Waveform

Radar Waveform

Comm Waveform

Radar Tx
Radar Rx
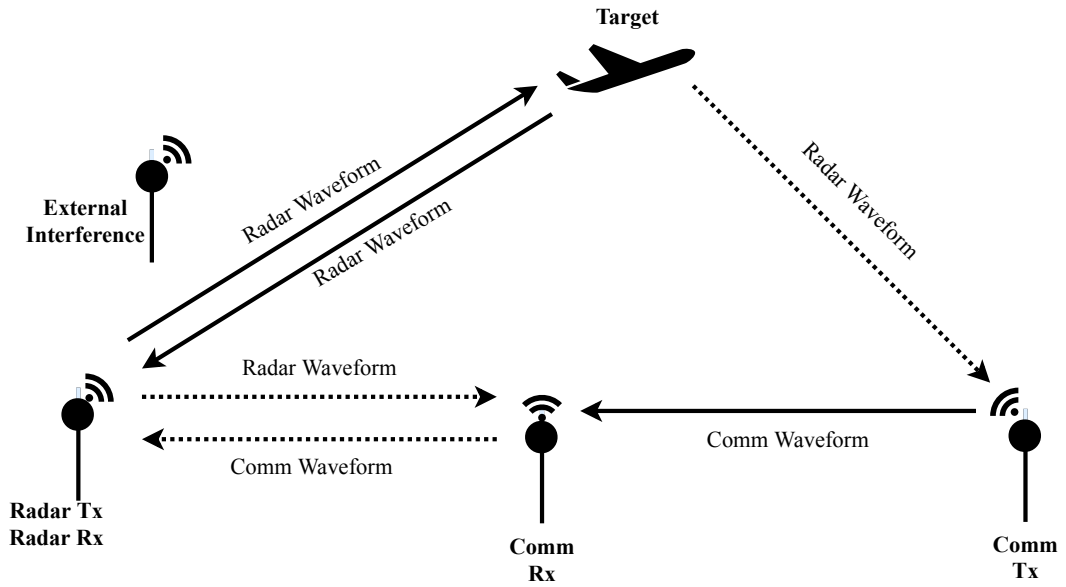
Comm
Rx

Comm
Tx

Figure 1.6: Radar system and the communication system designed in isolation.

new generation of dual communication and radar systems that can handle the trend towards less exclusionary spectrum policies and interference [21]. The frequency spectrum became one of the most valuable resources. The strictly limited spectrum resources leads to a better use of this resource exploiting the spectrum for opportunistic spectrum usage. One example is the design of a joint radar and communication (RadCom) system. This system caught the attention in many fields and it is already being extensively researched to take full advantage of the limited spectrum [16].

The idea of combining this two systems in one is not new [22],[23]. However, the existence of such systems is rare . NASA Space Shuttle "Orbiter" is one of the few examples, the system could switch between radar and communication but not perform the both at same time [24]. The true philosophy of joint radar and communication relies on embedding in the radar waveform the communication message [25],[26].

The potential strategies that may lead to the integration of communication and radar systems in the future include [16]:

- Intelligent signal coding like OFDM;

- MIMO;

- Digital beamforming;

- Array imaging;

- Combination of radar-communication (RadCom).

The use of OFDM as the supporting signal model to this kind of systems was first suggested in [27] and studied in [28],[29]. A collocated antenna architecture and a spectrum sharing algorithm for RadCom systems were suggested in [30] and a digital beamforming for a higher angular resolution in [31]. In this work, we consider the combination of OFDM multiple input multiple output (MIMO) technology and digital beamforming for the integration of radar and communication systems. These concepts are explained more deeply in the next chapters.

The integration of wireless communication and radar sensing systems will bring up many benefits in areas such as, intelligent transportation systems (ITS), wireless sensor networks (WSN) and modern military applications [32]. A typical application of such system can be found in the automotive field. A joint radar and communication systems for automotive systems, is already being discuss [33]. ITS require smart vehicles to have the capability of autonomously sensing the driving environment and cooperatively exchanging information data such as velocity and braking between vehicles and also road, traffic and weather conditions [32]. With self-driving cars, two technologies emerge as well, such as vehicle-to-vehicle (V2V) communications and navigational/avoidance radar [34],[35]. Figure 1.7 shows some communication scenarios in intelligent transportation systems.

In the current market, among the most popular smart cars we have the ones developed by Tesla Motor's. The autopilot mode developed by the Tesla Motor's relies on its sensors and learning algorithms. The car is capable of steer safely within a straight road, initiate lane

change, manage speed and park the car, but the system is not intelligent enough to react in more complicated traffic situation [36]. A vehicular network where the vehicles collaborate with each othe by providing their navigation and sensor information to other vehicles (V2V communications) would be beneficial to situations like this.
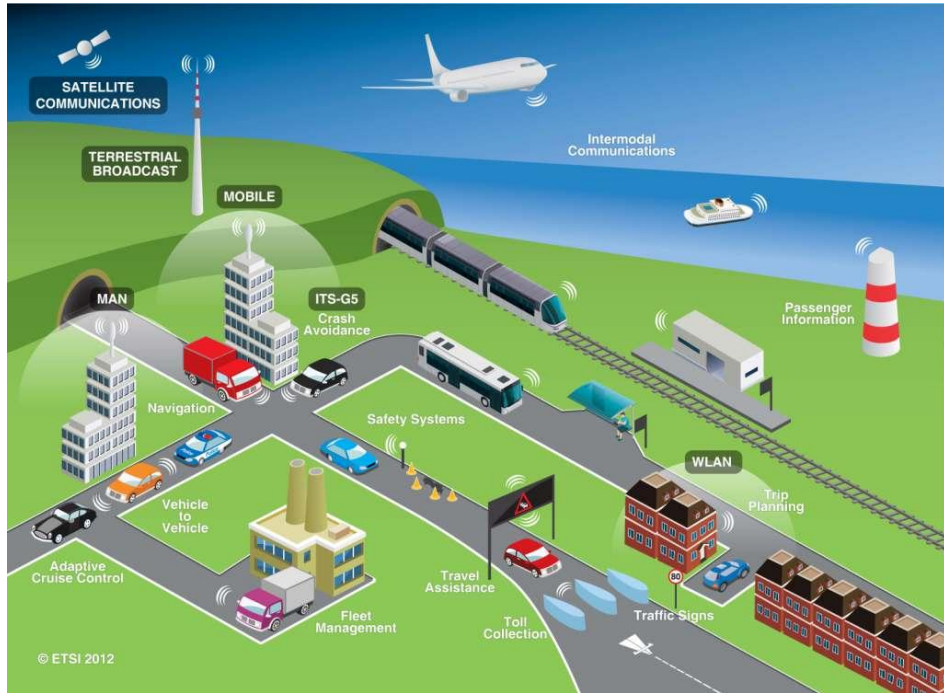
Figure 1.7: Intelligent Transportation Systems [37].

1.3 Overview and Motivations

Wireless mediums, such as RF, optical, or acoustical, provide finite resources for applications such as radar and communications systems. The two systems have been studied and developed separately. Often, they compete with one another for the same resources [34]. The design of a system that integrate both radar and communication functions in the same hardware can be beneficial in terms of cost, dimension, performance and spectral efficiency [38]. Moreover, to meet the increasing requirements on the radar performance, evolution in terms of signal processing algorithms as well as in the radar concept become more necessary. The spectrum congestion problem is forcing the research for cooperative methods and joint design approaches to accomplish the growing number of communication applications and the demand for high data rates [39].

The internet of things (IoT) will connect all kind of objects through the internet. The radar and communication technology are fundamental aspects that will also bring advantages for the future of Internet of things [40]. The growing number of radar applications led us to a need for presenting a more robust radar technology. One of the most important aspects of the radar technology is the signal modulation. A technology that gained attention in the last few years was the use of OFDM waveform for the radar [27]. The advantages of using

OFDM as signal brings to the radar system a better range resolution, spectral efficiency and frequency diversity. Furthermore, some studies considered the extension of OFDM radar to a multiple-input multiple-output (MIMO) radar system [41].

The main motivation of a joint radar and communication system goes to the efficient use of limited spectral resources based on a single waveform that combines both applications radar and communications [22][29][41]. This dissertation considers both the signal detection and wireless communication areas, having as main objective to evaluate the performance of an integrated radar and communication system. The specific objectives include:

1. The development of an OFDM Radar system, where the velocity and range parameters are estimated;

2. The incorporation of multiple antennas in the OFDM Radar system developed in order to be able to perform angle estimation;

3. The combination of the Alamouti Coding in the OFDM Radar to establish a communication link with another device, maintaining the radar functionality;

4. The performance evaluation of the proposed and developed systems by resorting to numerical simulations.

1.4 Contributions

The main contribution of this work is the combination of the Alamouti code with OFDM, which allowed the integration of radar and communication technologies in a simple and efficient way. Therefore, the application in practical systems is also interesting.

1.5 Structure

This dissertation starts by introducing the background of communication systems and its evolution, then an overview of joint radar and communication systems is performed, and some applications presented. Next, the motivations and objectives of this work are described and from this point onward, the dissertation structure is organized in the following form:

In chapter 2, the radar fundamentals are presented. The Chapter starts by explaining an elementary radar system and the main radar parameters. Additionally, the radar equation and the different types of waveform are studied. The frequency bands commonly used for the radar operation are also presented in this chapter.

In chapter 3, we briefly introduce the OFDM concept for communication systems, then study the use of OFDM for radar. The radar most important requirements for the design of radar systems are also presented in this chapter.

In chapter 4, we introduce the MIMO concept for the radar system. First, an overview of the main characteristics, for the communication technology, of MIMO systems such diversity and spatial multiplexing are made, then, specific antenna configurations for MIMO radar are presented. Finally, the OFDM MIMO signal model for radar applications is studied.

In chapter 5, we divide the chapter in three parts. First, the implemented OFDM MIMO Radar system is described, which includes the system model and the radar processing to obtain the radar image. Follows, the description of the method to combine the Alamouti code with OFDM to enable joint radar and communication. Finally, the performance results are presented.

The last Chapter presents the main conclusion of this work and points out possible future works.

Chapter 2

Radar Fundamentals

Radio Detection and Ranging (Radar) is an electromagnetic system to detect and locate objects. Detection and ranging have been and continues to be the primary function of radar. Modern radars do much more than just detection and ranging, they are able to find many characteristics about the target such as its size, shape and velocity, for example. This features of the radar system make them an important tool for military and civilian applications.

This chapter focuses on the radar fundamentals, including the radar functions, radar parameters and different radar types.

2.1　Radar Basics

The radar systems can be categorized as monostatic radar, where the transmitter and the receiver are located in the same place and bistatic radar where the transmitter and receiver are separated. This work studies only the monostatic radar. A simple form of radar starts by transmitting electromagnetic waves in all the directions. The targets in the environment intercept these radiated waves and reflect back in all directions. A part of this reflected signal is received by the radar system. The received signal is processed to obtain information about the target, like velocity and range. Figure 2.1 shows a typical radar scenario.

An elementary radar can be described by the block diagram illustrated in Figure 2.2. The radar signal generated by the waveform generator is modulated and sent to the power amplifier. The waveform is generated at a low power level, in order to generate different types of waveforms in an easier way for the different types of radars, then through a power amplifier the signal is raised to the desired power level. The duplexer allows the same antenna to be used for both transmitting and receiving. The duplexer acts as a switch disconnecting the receiver from the antenna and protecting the receiver from the high power when the transmitter is ON, to avoid damage. The duplexer also acts as a channel to the echo signal forwarding the signal to the receiver and not to the transmitter. The first stage of the receiver might be a low noise amplifier or it can be the mixer stage. Radars with a low noise amplifier in the first stage make the radar more sensitive, the input mixer can have greater dynamic range, less susceptibility to overload, and less vulnerability to electronic interference. Radar without a low noise amplifier is used especially in military radars that must operate in a noisy environment.
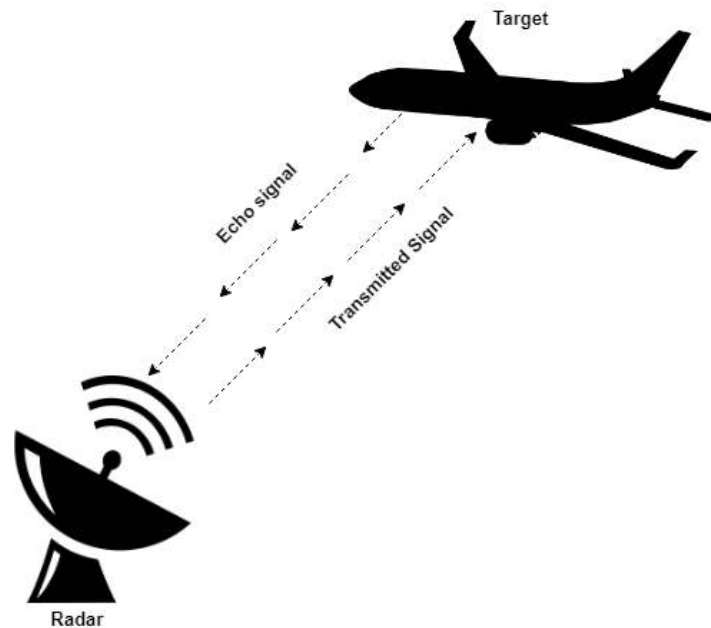
Figure 2.1: Radar scenario.

The receiver amplifies the reflected signal to a level where it can be easily analyzed. The local oscillator and mixer are used to convert the received RF signal to the intermediate frequency signal. The matched filter should maximize the signal-to-noise ratio at the output for signal processing. It should separate the desired signal from the clutter signal portion. After maximizing the signal-to-noise ratio, the modulated signal is extracted by the second detector and amplified by the video amplifier and displayed.
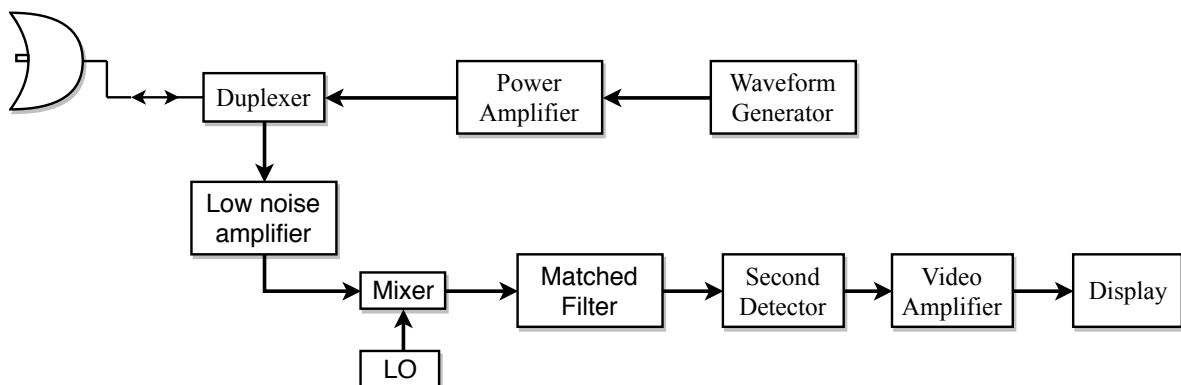
Figure 2.2: Block diagram of a Radar.

2.1.1 Radar Functions

Some of the basic functions performed by the radar include target detection, target velocity and determining the range. These functions will be briefly described in this section. Some of the parameters listed cannot be performed by some types of radar, depending on the waveform used by the radar as we will see in section 2.4.

Target detection

Detection is the process of determining whether or not a target is present. There are four possible conditions of detection[42]. Figure 2.3 illustrates the possibilities. In (a) the target is present and detection occurs, the result is considered correct. In (b) there is no target and the radar display also shows no detection, the result is correct. In (c) there is the presence of a target and the radar fails to show it on the display, an error occurs. In (d) there is no presence of a target and the radar shows detection, in this case the error occurred is referred to as a false alarm. These errors normally occur because a weak target can be confused by a strong interference.
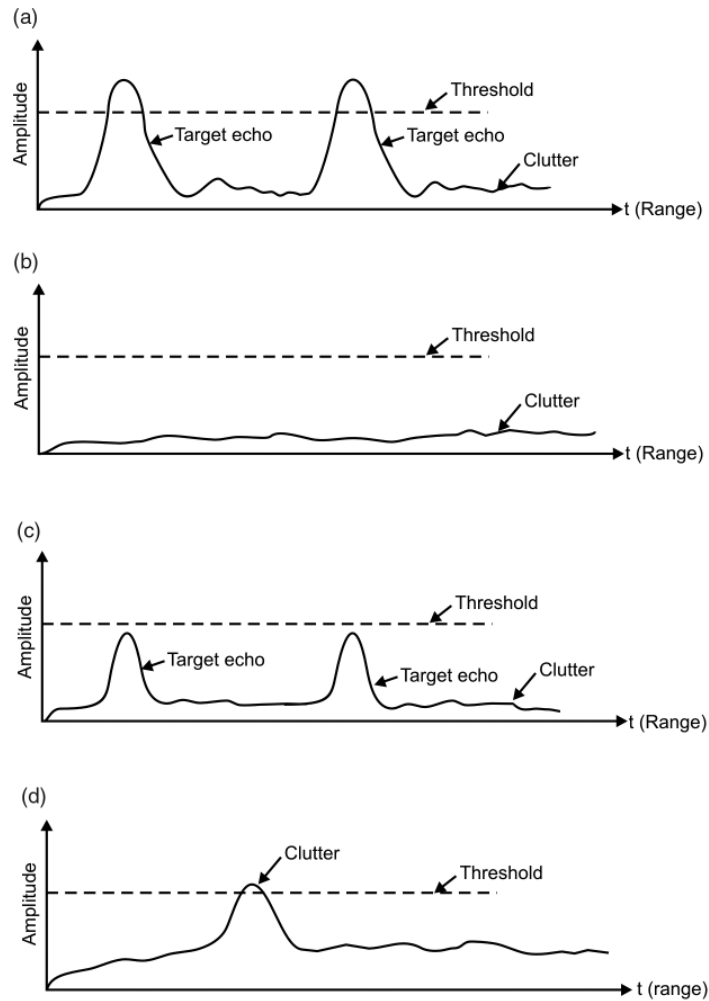
Figure 2.3: The conditions of detection[42].

Range and delay

The range is used to indicate the distance between the radar system and the target. In radar, time synchronization is required for the transmission of radar signals that are measured by the range of radar [43]. So due to the modulation of the transmitted signal, the time taken by the wave to travel to the target and back to the radar can be measured.

13

Assuming t_d to be the round trip time from the radar to the target and back to the radar, and assuming that the propagation velocity c_0 of the electromagnetic wave is equal to the speed of the light ($c_0 = 3 \times 10^8 m/s$). The relation between the round trip time (t_d) and the range (R) is,

$$R = \frac{t_d c_0}{2}.$$ (2.1)

R is in meters and t_d is in seconds. The fraction $1/2$ is due the round trip travel time.

Range resolution

The range resolution is the ability of the radar to distinguish between targets that are close to each other in range. The radar resolution depends on the pulse width that is also related to the signal bandwidth. The equation that expresses how close two targets can be in range to be distinguished can be given by

$$\Delta R = \frac{c_0 \tau}{2} \frac{c_0}{2B}$$ (2.2)

Figure 2.4 shows a practical scenario.
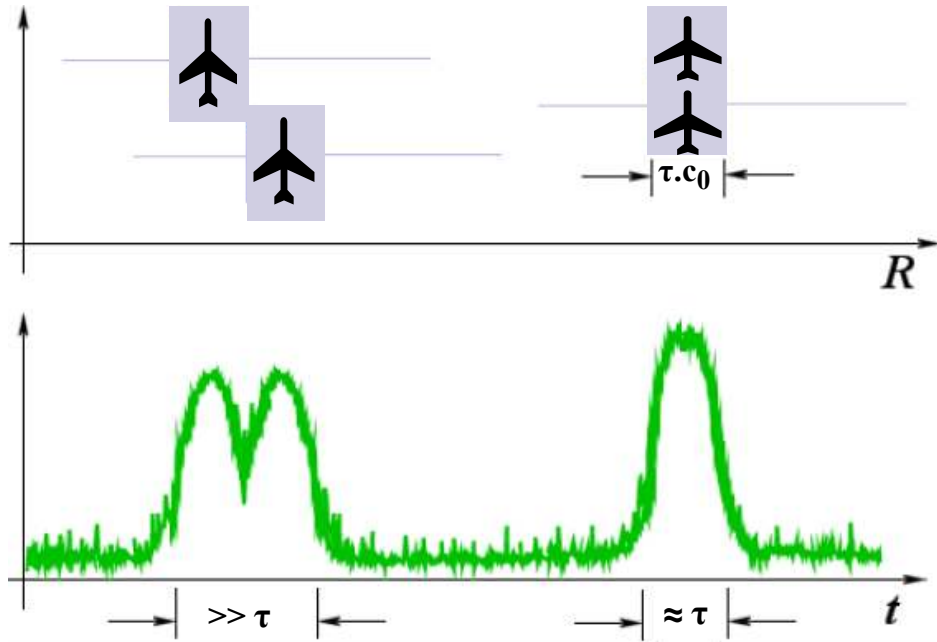
Figure 2.4: Minimum distance of targets in range [44].

Velocity and Doppler effect

Radars use the Doppler effect to estimate the relative velocity. The Doppler effect can be translated into a change in the frequency or wavelength of the wave in relation to an observer who is moving relative to the wave source [45]. Figure 2.5 shows an example.
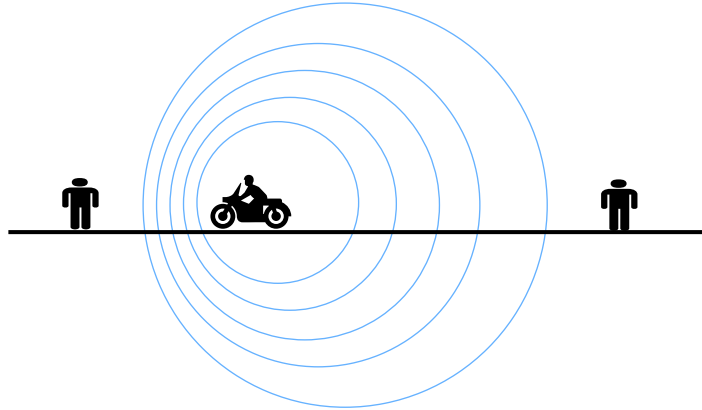
Figure 2.5: Doppler effect.

The Doppler effect is related to radial velocity as

$$f_D = \frac{\pm 2v}{\lambda} \tag{2.3}$$

The Doppler shift is inversely proportional to wavelength λ, and its sign is positive or negative, depending on whether the target is approaching or moving away from the radar.

Doppler resolution

The Doppler resolution is the ability of the radar to distinguish targets with different radial velocities in the same range. The Doppler resolution can be express as

$$\Delta f_D = \frac{1}{T_{obs}} \tag{2.4}$$

where T_{obs} is the observation time.

2.2   Frequency Band

Radar frequency bands are classified into letter designations standardized by the Institute of Electrical and Electronic Engineering (IEEE) in [46]. The most commonly used bands operate in a range of 220 MHz to 35 GHz[47]. Table 2.1 shows the different frequency bands and their nomenclature.

Table 2.1: Frequency bands [46].

Band designation	Frequency Range	Applications
HF	3 - 30 MHz	Over-the-horizon surveillance
VHF	30 - 300 MHz	Long-range air surveillance
UHF	300 - 1000 MHz	Long-range air surveillance, Ground penetrating RADAR
L	1 - 2 GHz	Long-range air surveillance
S	2 - 4 GHz	Medium-range air surveillance
C	4 - 8 GHz	Medium-range air surveillance, Long-range tracking
X	8 - 12 GHz	Short-range tracking, Missile guidance
Ku	12 - 18 GHz	High resolution mapping
K	18 - 27 GHz	Weather
Ka	27 - 40 GHz	Very high resolution mapping
V	40 - 75 GHz	-
W	75 - 110 GHz	Automotive
mm	110 - 300 GHz	-

2.3   Radar equation

The radar equation is a deterministic model that relates received echo power to transmitted power in terms of a variety of system design parameters. The radar equation also relates the characteristics of the transmitter, receiver, antenna, target, and environment[48] [49]. In this section, the simple form of radar equation is described.

Assume that an isotropic radiating element transmits a waveform of power P_t and no power is lost in the medium, the power density at a range R is the total power P_t divided by the surface area of a sphere of radius R [49],

$$Power\,density\,from\,isotropic\,antenna = \frac{P_t}{4\pi R^2}\ \ W/m^2 \tag{2.5}$$

Radars employ directive antennas to focus the outgoing energy in the direction of the target. The increased power radiated in a particular direction has a gain G associated to the antenna,

$$Power\,density\,from\,directive\,antenna = \frac{P_t G}{4\pi R^2}\ \ W/m^2 \tag{2.6}$$

A target at range R intercepts a portion of the incident power and radiates it in various directions, some part toward the radar. The part power radiated back to the radar is denoted as the radar cross section δ, the relation is given by

$$Power\,density\,of\,echo\,signal\,at\,radar = \frac{P_t G}{4\pi R^2}\frac{\delta}{4\pi R^2}\ \ W/m^2 \tag{2.7}$$

If the effective area of the receiving antenna is denoted A_e, the power P_r received by the

radar is

$$P_r = \frac{P_t G}{4\pi R^2} \frac{\delta}{4\pi R^2} A_e \quad W \tag{2.8}$$

Being,

$$A_e = \frac{\lambda^2 G}{4\pi} \tag{2.9}$$

The radar system suffers from very large signal path losses. There are losses associated with the radar cross section, the reflexibility of targets and the round-trip distance is twice that of a general communication system.

The maximum radar range R_{max} is the distance beyond which the target cannot be detected. It occurs when the received echo signal power P_r just equals the minimum detectable signal S_{min}[48].

$$R_{max} = \left[\frac{P_t G_t A_e \delta}{(4\pi)^2 S_{min}} \right]^{\frac{1}{4}} \tag{2.10}$$

In practice, the observed maximum radar ranges are usually much smaller because some factors that affect range are not explicitly included in the equations above.

The minimum detectable signal, S_{min} is limited by receiver noise and can be expressed as

$$S_{min} = kT_0 B F_n \left(\frac{S}{N} \right)_{min} \tag{2.11}$$

where k is the Boltzmann constant, T_0 is the temperature, B is the receiver bandwidth, F_n is the noise factor and $(\frac{S}{N})_{min}$ the minimum value of signal-to-noise-ratio.

Noise Factor

The noise power in practical receivers is often greater than can be accounted by thermal noise alone. The additional noise components are due to a mechanism other than the thermal agitation of the conduction electrons. The total noise at the output of the receiver may be considered to be equal to the thermal-noise power obtained from an "ideal" receiver multiplied by a factor called the noise factor or noise figure[48]. The factor noise is defined by the equation

$$F_n = \frac{N_0}{kT_0 B G_n} \tag{2.12}$$

where N_0 is the output noise from the receiver, G_n the available gain.

Radar Cross Section

The radar cross section (RCS) can be express as

$$\delta = 4\pi R^2 \frac{|E_r|^2}{|E_t|^2}, \tag{2.13}$$

and represents the magnitude of the reflected signal to the radar by the target. E_r is the electric field strength of the reflected signal at the radar and E_t the electric field strength incident on the object.

2.4 Radar Waveform

The type of waveform employed by a radar is a major factor that affects the radar system performance metrics, such as range resolution, velocity resolution, SNR, and the probability of target detection[50]. Radar systems can be divided into two classes according to the waveform used: continuous wave (CW) and pulsed. Both pulsed and CW waveforms can be further categorized based on the presence or absence of frequency or phase modulation.

2.4.1 CW Waveform

With CW waveform the transmitter is continually transmitting a signal, while the radar transmitter is operating. The receiver continuously operates also. Due to the constraints of continuous RF power, the detection range is relatively short. CW waveforms have the highest Doppler sensitivities but no range resolving power[51]. Since a single frequency unmodulated signal using by a CW radar cannot measure the target range, the wave must be accomplished with a frequency modulation (FM). This technique puts a timing mark on the electromagnetic wave. The modulation signal could be a sine or a triangle as shows the Figure 2.6.
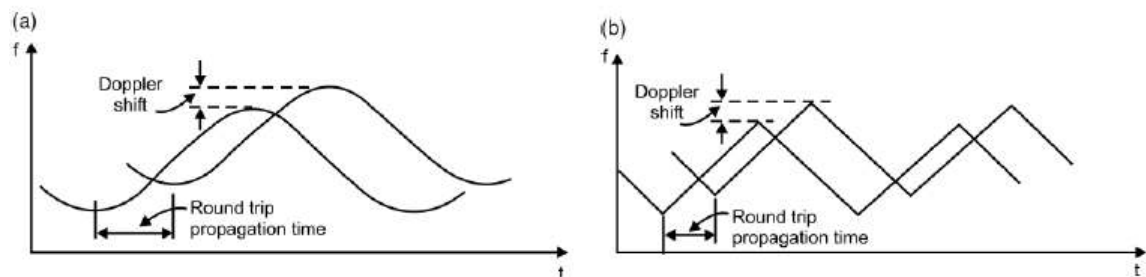
Figure 2.6: (a) Sine wave modulation and (b) triangular modulation [42]

2.4.2 Pulsed Waveform

Pulsed radars transmit EM waves during a very short time duration, or pulse width τ, typically 0.1 to 10 microseconds(μs) [52]. Pulsed waveforms can be defined based on a single pulse. Figure 2.7 shows some common pulsed radar waveforms.
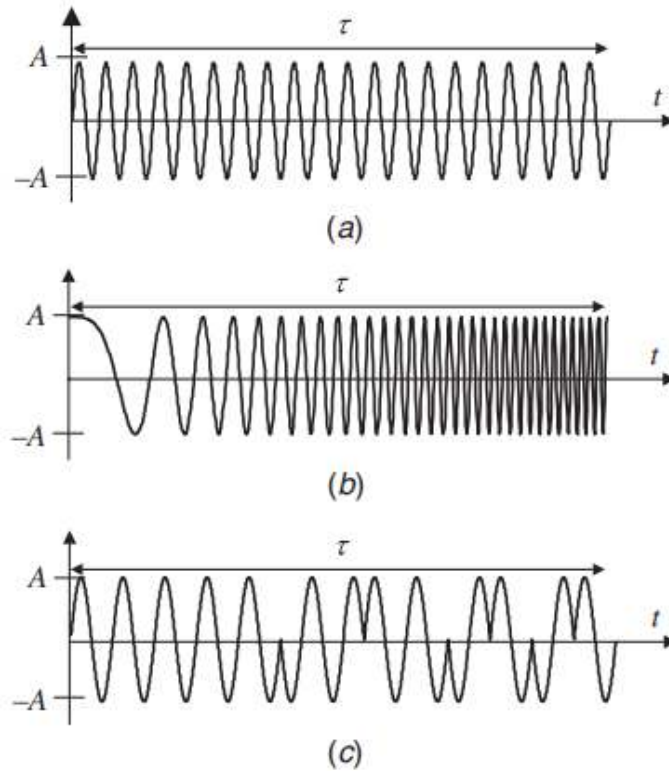
Figure 2.7: (a) simple pulse, (b) linear frequency modulated, (c) binary phase-coded pulse [52]

During the pulse transmission time, the receiver can not detect any signal and while the transmitter is off, the receiver is on so that target signals can be detected. The pulsed waveform is illustrated in Figure 2.8.
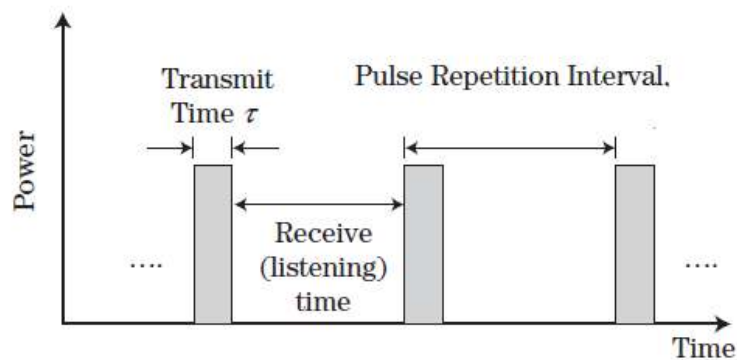
Figure 2.8: Pulsed radar waveform [52]

The radar waveforms, are summarized in Table (2.2) and Table (2.3) [50].

19

Waveform Type	Transmit Waveform	Detection Principle
CW	$e^{j2\pi f_c t}$	Conjugate mixing
Pulsed	$\prod(T_p)e^{j2\pi f_c t}$	Correlation
FMCW	$e^{j2\pi(f_c t + 0.5Kt)t}, K = \frac{B}{T_0}$	Conjugate mixing
SFCW	$e^{j2\pi f_n t}, f_n = f_c + (n-1)\Delta f$	Inverse Fourier transform
OFDM	$\sum_{n=0}^{N-1} I(n)e^{j2\pi(f_c t + n\Delta f)t}$	Frequency domain channel estimation

Table 2.2: Radar Waveforms-Transmit Waveform and Detection Principle.

Waveform Type	Resolution	Comments
CW	$\Delta f_d = 1/T;$	No range information
Pulsed	$\Delta R = cT_p/2; \Delta f_d = 1/T_p$	Range-Doppler performance tradeoff
FMCW	$\Delta R = c/2B; \Delta f_d = 1/PT_0$	Both range and Doppler information
SFCW	$\Delta R = c/2B; \Delta f_d = 1/PT_0$	Δf decides maximum range
OFDM	$\Delta R = c/N\Delta f; \Delta f_d = 1/PT_N$	Suitable for vehicular communication

Table 2.3: Radar Waveforms-Resolution.

In Table (2.2) and Table (2.3) :

- B denotes bandwidth of the radar.

- T is the amount of time for which data is captured.

- N stands for a number of samples in CW and number of carriers in OFDM.

- $\prod(T_p)$ is a rectangular pulse of duration T_p.

- P is the number of FMCW/SFCW or OFDM blocks of duration T_0 and T_N, respectively.

- $I(n)$ is an arbitrary sequence and Δf is carrier/frequency separation in OFDM/SFCW.

Chapter 3

OFDM Radar Systems

To perform the integration of radar and communication a feasible option is do this using an integrated waveform. The design of an integrated waveform can be classified into two main categories, the use of multiplexing techniques or the use of waveform sharing[53]. The idea is hidden in the traditional radar, the payload data.

There have been many types of research regarding orthogonal frequency division multiplexing(OFDM) as a waveform suitable to perform radar functions and communication functions [54],[55]. OFDM is mostly used as a communication signal, whereas it is uncommon for radar systems. Amplitudes and phases of carriers constituting the OFDM signal carry the communication message. For radar systems, the process of getting the important information from the signal passes to the matched filtering. The matched filtering is the calculation of the correlation of the received echo with the transmitted radar signal in an effort to minimize the additive white Gaussian noise [56].

This section discusses the concepts of the OFDM waveform, and the OFDM as the radar signal.

3.1   OFDM Signal Basics

The basic principle of OFDM is to split a high-rate datastream into a number of lower rate streams that are transmitted simultaneously over a number of sub-carriers[57], as represented in Figure 3.1. The carriers that constituting the signal are uniformly spaced in frequency, being mathematically orthogonal. Firstly, to generate multiple carriers was through a bank of shaping filters which provided the orthogonality between the carriers [58]. Filter banks are an array of band-pass filters that separate the input signal into multiple components. The implementation of the OFDM with a large number of carriers was not practical based on the filter banks, so lately the filter banks were replaced with the fast Fourier transform(FFT) algorithms[59]. In this work the OFDM generated and the demodulated are through IFFT and FFT respectively.
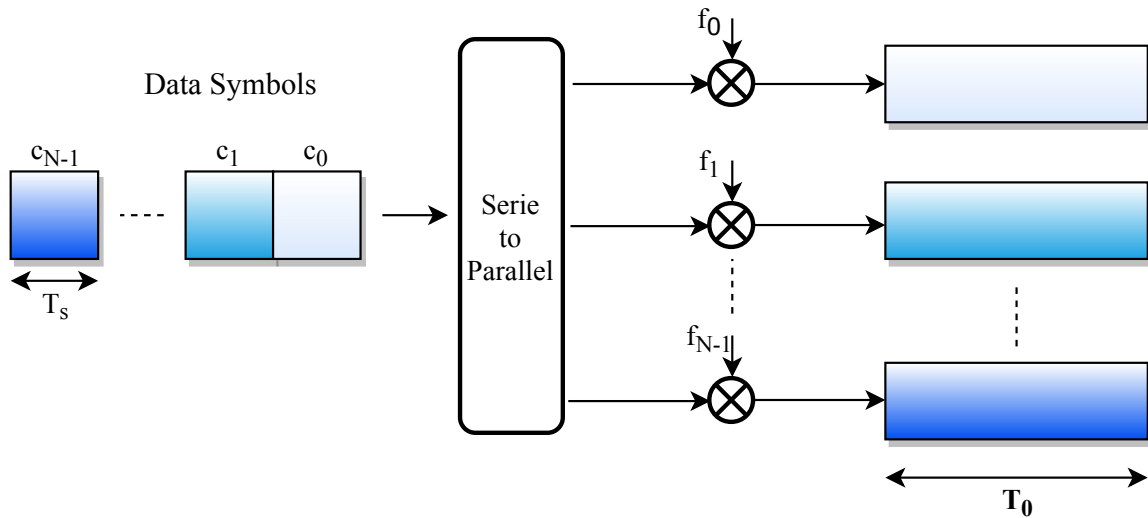
Figure 3.1: OFDM modulation.

OFDM is widely adopted because of a number of advantages that it offers[60]:

- Orthogonality of sub-carriers signals that allow:

  - trivial generation of transmit signal through an IFFT block;
  - trivial separation of the transmitted data symbols at the receiver through a FFT block;
  - trivial adopting to multiple-input multiple-output(MIMO) channels.

- Adaptive modulation schemes can be applied to sub-carrier bans to maximize the bandwidth efficiency.

- The structure of OFDM symbols simplifies the task of carrier and symbol synchronization.

3.1.1 Signal Generation

The OFDM signal can be visualized as a set of signals spanning a bandwidth, all modulated onto non-overlapping sub-carrier frequencies, as showed in Figure 3.2 .
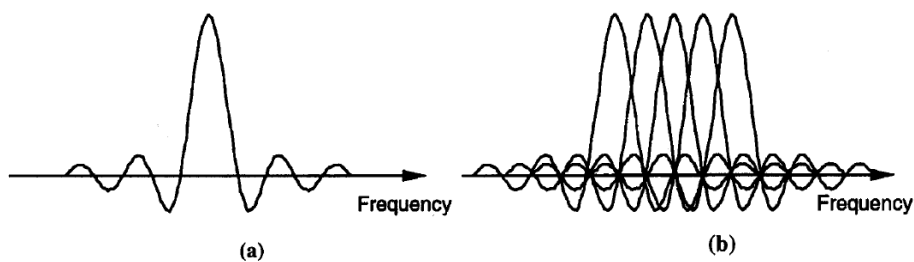
Figure 3.2: Spectra of (a) an OFDM sub-channel and (b) an OFDM signal [57].

The sum of sub-carriers that constituting the OFDM signal are modulated using phase shift keying (PSK) or quadrature amplitude modulation(QAM). Assuming c_k to be the complex symbol transmitted, each one modulated in one different sub-carrier, with a frequency associated, f_0 through f_{N-1}, T the symbol duration and f_c the carrier frequency of the entire signal. The orthogonality is ensured by choosing a constant sub-carrier spacing, that corresponds to the inverse of the OFDM symbol duration,

$$\Delta f = \frac{1}{T} = \frac{B}{N}. \tag{3.1}$$

Figure 3.3 shows the OFDM signal in the time-frequency plane.
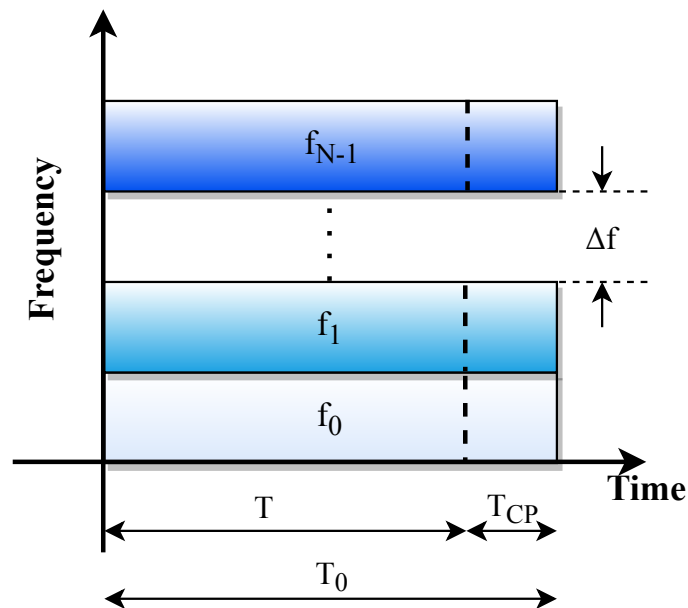
Figure 3.3: An OFDM block in the time-frequency plane.

A set of modulation symbols transmitted in the same time slot is called an OFDM symbol. An OFDM signal can have a total of M time slots. The group of N signals, for each OFDM symbol form a frame with dimension $N \times M$. Figure 3.4 illustrates the distribution of the information at the OFDM frame.
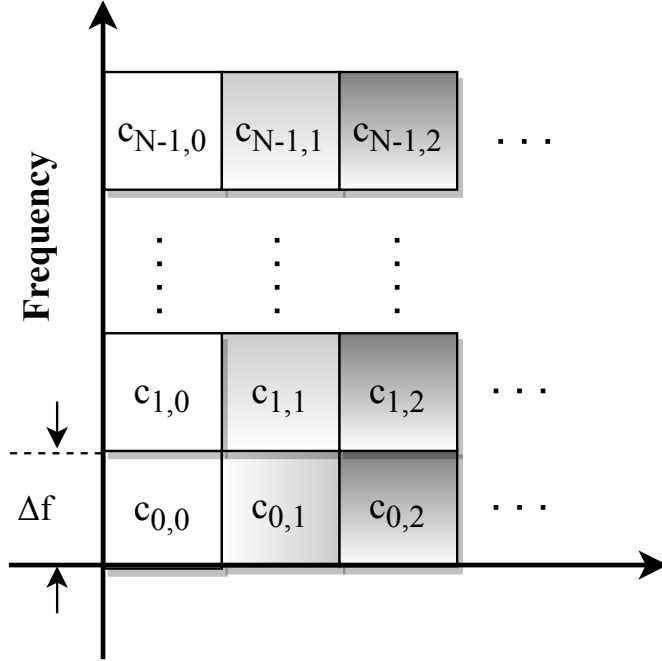
Figure 3.4: OFDM frame schematic.

Assuming a rectangular pulse shape of duration T for the modulation symbol $c_{k,l}$,

$$rect(t) = \begin{cases} 1, & 0 \leq t < T \\ 0, & otherwise \end{cases} \tag{3.2}$$

the mathematical expression for the complex baseband OFDM signal correspondent to one 0-*th* OFDM symbol is given by,

$$s(t) = rect(t) \sum_{k=0}^{N-1} c_{k,0} e^{j2\pi k \Delta f t}. \tag{3.3}$$

The OFDM signal can efficiently be performed using an inverse fast Fourier transform (IFFT) before the transmission. Considering the length of the IFFT equal to the total number of sub-carriers and replacing the time variable by the sampling period,

$$t = n\frac{T}{N} = \frac{n}{N\Delta f} \tag{3.4}$$

The discrete version of the signal on the 0-th OFDM symbol is given by,

$$s(n) = s(nT/N) = \sum_{k=0}^{N-1} c_{k,0} e^{j2\pi k \frac{n}{N}}, \; n = \{0, 1, ..., N-1\}. \tag{3.5}$$

The original sequence c_k can be recovered by sampling it at a rate N/T, and applying the FFT over the N samples from on slot with duration T [61].

$$[s_n] = IFFT[c_k] \Rightarrow [c_k] = FFT[s_n]. \tag{3.6}$$

24

3.1.2 Orthogonality

Orthogonality is a property that allows multiple information signals to be transmitted perfectly over a common channel and detected, without interference. Loss of orthogonality results in blurring between these information signals and degradation in communications[62]. Sets of functions are orthogonal to each other if they match the next condition

$$\int_0^T s_i(t)s_j(t)dt = \begin{cases} C & i = j \\ 0 & i \neq j \end{cases} \tag{3.7}$$

In the frequency domain, each OFDM subcarrier has a *sinc*, frequency response. The *sinc* shape has a narrow main lobe, with many side-lobes that decay slowly with the magnitude. Each carrier has a peak at the center frequency and the peak of each subcarrier corresponds to the nulls of all other subcarriers as the Figure 3.5 illustrates.
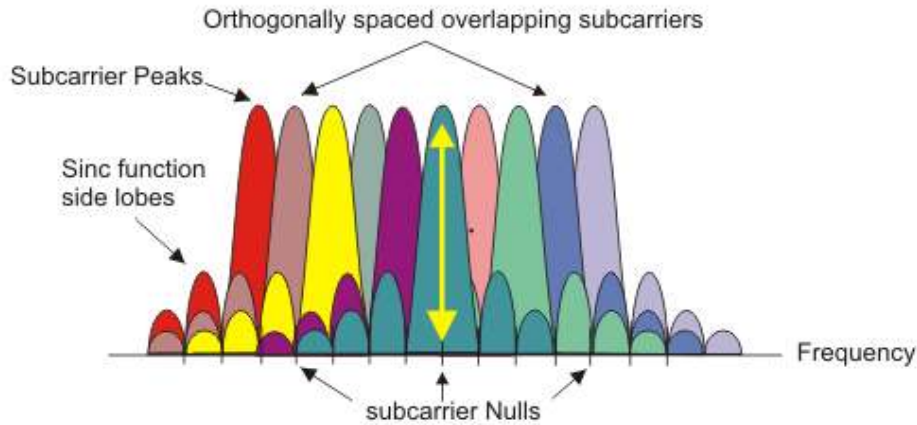
Figure 3.5: OFDM signal frequency spectrum [63]

3.1.3 Cyclic Prefix

The transmitted OFDM symbol can be received with distortion due to multipath propagation. Multipath propagation is caused by the radio transmission signal reflecting off objects in the propagation environment[62]. This spreads the symbol boundaries causing inter-symbol interference (ISI).

To eliminate the inter-symbol interference a guard interval is inserted before every OFDM symbol. The creation of the guard interval can be made by copying the last part T_{CP}/T part of the OFDM symbol. This cyclic copy extends the length of the symbol waveform to $T_0 = T + T_{CP}$. The duration of T_{CP} normally is chosen according to $T_{CP}/T = 1/4$ or $T_{CP}/T = 1/8$.

Figure 3.6 shows the method of introducing the cyclic prefix (CP) by coping a piece of the OFDM symbol and put it in front of the signal.
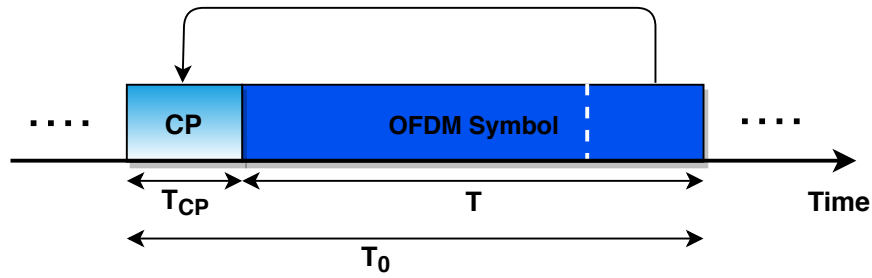
Figure 3.6: Cyclic Prefix.

3.1.4 The OFDM System

Figure 3.7 shows a schematic of an OFDM transmitter and receiver. In this work, the parameters related to the RF front-end are ignored. At the transmitter side, the first step is to modulate the message into symbols, using Phase Shift Keying(PSK) or quadrature amplitude modulation(QAM). Then, the flow of complex symbols is converted from serial to parallel, and each phase code is attributed to each subcarrier. An inverse discrete Fourier transform(IFFT) is applied. The discrete time signal resulting from the IFFT is converted from parallel to serial and as result the discrete time domain of the OFDM symbol is defined. In the end the cyclic prefix is added.
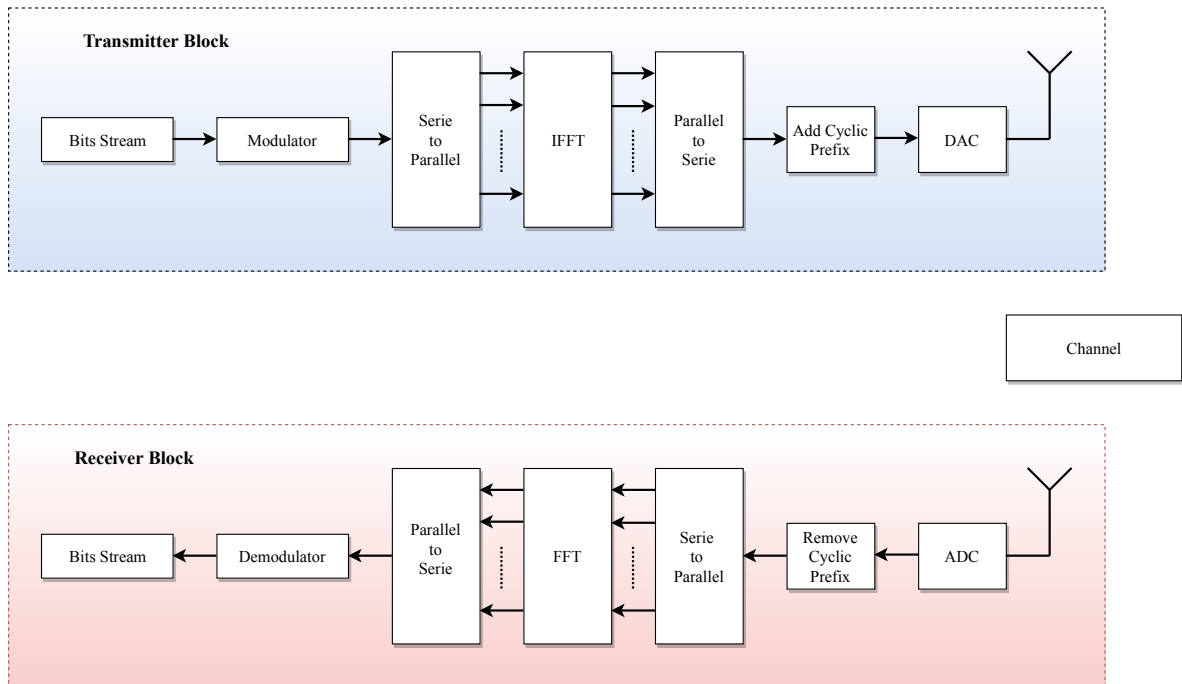
Figure 3.7: OFDM architecture block diagram.

At the receiver side, first the cyclic prefix (CP) is removed, then the OFDM symbol is converted from serial to parallel and symmetrically to what happened in the transmitter, a fast Fourier transform(FFT) is applied. After the parallel-to-serial conversion and the demodulation, the message is recovered. Table 3.1 shows a list of relevant parameters.

26

Symbol	Parameter
N	Number of subcarriers
M	Number of OFDM symbols
B	Signal bandwidth
Δf	Subcarriers spacing
T	OFDM symbol duration
T_{CP}	Duration of the cyclic prefix
T_0	Total duration of OFDM symbol
$N_{Total} = N$	IFFT length
$M_{Total} = M$	FFT length
f_c	Carrier frequency
$f_s = N_{Total}\Delta f$	Sampling rate

Table 3.1: OFDM parameters.

3.1.5 Communication Requirements

In communication the main restrictions are imposed by the characteristics of the wave propagation channel. Given a multipath propagation channel, the signal parameterization must be chosen such that there is neither interference between consecutive OFDM symbols(ISI) nor between adjacent sub-carriers (ICI).

Consider the following characteristics of propagation channels for OFDM [64]:

- The maximum excess delay τ_e. Radio waves usually reach the receiver on a variety of paths, and arrive at different times. The time difference between the first and the last arrival of the same wave is described by τ_e

- The Doppler spread B_D. This describes the widening of the spectrum, caused by different Doppler shifts on each multipath. It is inversely proportional to the coherence time T_C, which is the time over which the channel may be assumed constant.

- The delay spread τ_{DS}, is an average value for the time difference of multipath propagation times. Paths are weighted by their attenuation, meaning that paths carrying more energy contribute more to tau_{DS} than paths with large fading. The delay spread is inversely proportional to the coherence bandwidth B_C, which is the bandwidth over which a channel may be considered flat.

The key parameters of the OFDM modulator system are the length of the guard interval T_{CP}, the carrier distance Δf and the number of carriers N [65]. The OFDM system needs to satisfy some conditions according to the characteristics above present.

First, the guard interval length needs to be larger than the maximum excess delay of the channel,

$$T_{CP} > \tau_e \tag{3.8}$$

i.e. the time difference between the arrival of the first and the last multipath signal. This simple condition can avoid the ISI.

Second, to avoid ICI, it is important that the subcarrier spacing is chosen larger than the Doppler spread and smaller than the coherence bandwidth of the channel,

$$B_D \ll \Delta f \ll B_C \tag{3.9}$$

in order to prevent the spreading destroy the orthogonality between carriers.

Lastly, the coherence time T_C of the channel must not exceed the symbol duration T.

$$T < T_C \ , \ \Delta f > \frac{1}{T_C} \tag{3.10}$$

3.2 OFDM signal as the Radar Signal

The radar operation can be described as the retrieval of target parameters from the received echo signal, like range and the radial velocity of a target.

There are two major features of OFDM signals which make it applicable in radar applications, which are the signal long duration and the wide spectrum. The first one, signal long duration helps to determine Doppler shift very accurately. On the other hand, the wide spectrum of the signal gives an opportunity to find a time shift of the received echo signal. Knowing these two values we can determine the velocity of the target and its distance from the radar system [66]. Several methods of OFDM radar signal processing have been proposed. One of the approaches was designed by using a correlation of received and transmitted signals [27]. In [67],[68] a novel approach is proposed which operates directly on the modulated symbols.
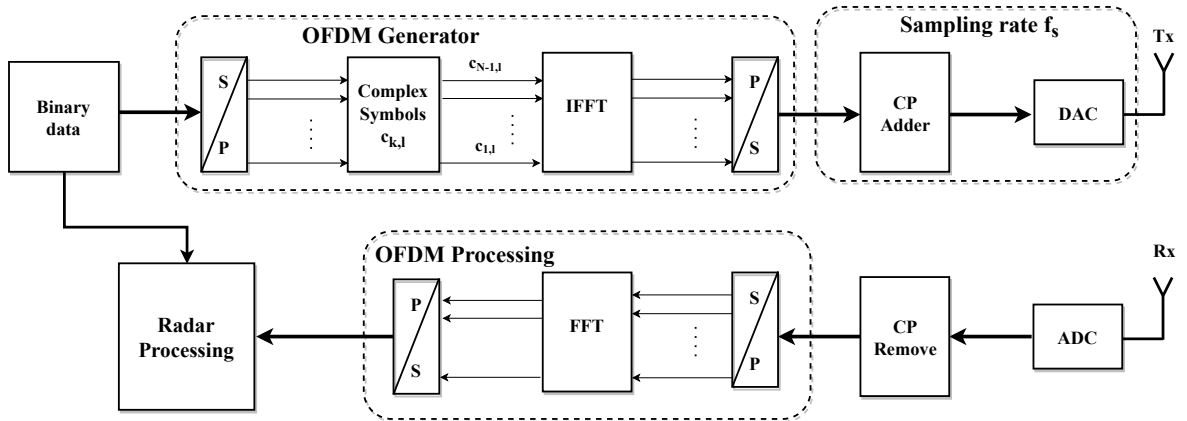
Figure 3.8: Block diagram of an OFDM Radar.

To use the OFDM communication signal for radio detection and ranging of the targets the baseband OFDM signal is modified to include the RF carrier frequency. To start, let us consider a SISO radar, whereby there is only one Tx and Rx pair on the same platform. The Tx and Rx are collocated at a distance d_{ant}, sufficiently smaller than their distance to the target which is in far-field region. The block diagram of a OFDM Radar system is presented in Figure 3.8. The radar transmits a signal $s(t)$ in the time domain and it can be represented

28

as [54][31]

$$s(t) = \sum_{l=0}^{M-1} \sum_{k=0}^{N-1} c_{k,l} \mathrm{e}^{j2\pi k\Delta ft} rect\left(\frac{t-lT}{T}\right). \tag{3.11}$$

The equation (3.11) says that each modulation symbol $c_{k,l}$ is modulated onto the subcarrier with the index k. The function $rect\left(\frac{t-lT}{T}\right)$ is a rectangular function with the duration of lT correspondent to every l-th OFDM symbol in the time domain. The CP is not shown for simplicity since it will be removed before the radar processing and will not affect the outcome of the radar estimation.

Considering the scenario illustrated in Figure 3.9. Assuming a total number of H targets, each located at the distance r_h. The wave $s(t)$ hits the objects and it is then backscattered to the radar. The total distance traveled by the signal can be assumed as $2r_h$, since $d_{ant} \ll r_h$. The time delay becomes a phase rotation when the Fourier transformed is performed according to

$$s(t-\tau) \implies S(f) \cdot \mathrm{e}^{-j2\pi f\tau}. \tag{3.12}$$
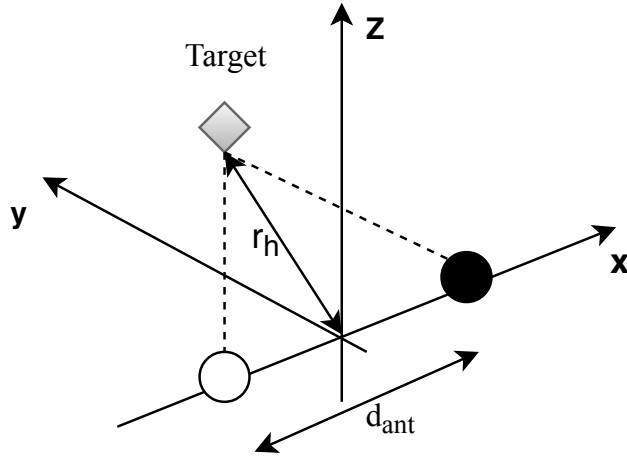
Figure 3.9: Radar scenario.

Considering a moving object, with a radial velocity v, which results in the Doppler frequency of f_D the OFDM signal reflected from a point target at range R is

$$r(t) = \sum_{h=0}^{H-1} b_h \mathrm{e}^{j\zeta} \sum_{l=0}^{M-1} \sum_{k=0}^{N-1} c_{k,l} \mathrm{e}^{j2\pi(k\Delta f+f_{D,h})(t-\tau_h)} rect\left(\frac{t-\tau_h-lT}{T}\right) + w(t) \tag{3.13}$$

As the carrier frequency is normally in the GHz range, which is much larger than the baseband subcarrier spacing, it is assumed that the Doppler term affects all subcarriers by an equal amount, then, the term $\mathrm{e}^{-j2\pi f_D \tau_h}$ can be neglected. The received OFDM signal can

29

be rewritten as

$$r(t) = \sum_{h=0}^{H-1} b_h e^{j\zeta} \sum_{l=0}^{M-1} \sum_{k=0}^{N-1} c_{k,l} e^{j2\pi(k\Delta f(t-\tau_h))} e^{j2\pi f_{D,h}t} rect\left(\frac{t-\tau_h-lT}{T}\right) + w(t) \qquad (3.14)$$

The equation (3.14) include the following effects:

- Every signal is attenuated by a factor b_h. The attenuation is

$$b_h = \sqrt{\frac{c_0 \sigma_{RCS,h}}{(4\pi)^3 r_h^4 f_C^2}}, \qquad (3.15)$$

- $e^{j\zeta}$ accounts for any random phase offset due to the state of the channel or hardware and is hence a complex value.

- The time that takes to travel to the object and back delays the signal by,

$$\tau_h = 2\frac{r_h}{c_0}. \qquad (3.16)$$

- The relative velocity $v_{rel,h}$ of the object cause a Doppler shift of the signal by,

$$f_{D,h} = 2\frac{v_h}{c_0} f_C. \qquad (3.17)$$

- w(t) represent the white Gaussian noise.

The received signal is to be processed in the digital domain. So, the discrete form is obtained by setting t equal to

$$t = \frac{nT}{N} + lT \qquad (3.18)$$

where n is the sample number, $n = 0, ..., N-1$.
The equation (3.14) can be rewritten as

$$r(k,l) = \sum_{h=0}^{H-1} b_h e^{j\zeta} c_{k,l} e^{-j2\pi k\Delta f\tau_h} e^{j2\pi f_{D,h}lT} + w(k,l) \qquad (3.19)$$

The evaluation of the range and velocity of the targets can be done by comparing the transmit and receive signals to extract the differences.

3.2.1 Radar Requirements

In order to guarantee reliable system performance, several criteria have to be considered when choosing the system parameters. This concerns in particular the effects that cause signal distortion like Doppler shift and multi-path propagation [68]. The OFDM signal specifications for joint radar and communications, was discussed in [65] and in [69].

Maximum unambiguous range

The r_{max} refers to the theoretical maximum possible target distance detectable by the radar without ambiguity. The radar range is periodic in time with a periodicity equal to the OFDM symbol duration [68]. Considering that the signal travels the distance twice, this results in a maximum unambiguous measurement distance of

$$r_{max} = \frac{c_0}{2\Delta f} = \frac{T c_0}{2} \tag{3.20}$$

Given the maximum detection range r_{max}, the guard interval is bounded by[52]

$$T_{CP} \geq \frac{2r_{max}}{c_0} \tag{3.21}$$

Range resolution

The range resolution gives us the minimum distance required between two objects to distinguish the objects as separate. The achievable range resolution of a radar system depends purely on the total bandwidth occupied by the transmitted signal [70]. It is expressed as

$$\Delta r = \frac{c_0}{2B} = \frac{c_0}{2N\Delta f} \tag{3.22}$$

Higher bandwidth means higher resolution. Given a maximum tolerable resolution Δr_{max}, this constrains the bandwidth to

$$B \geq \frac{c_0}{2\Delta r_{max}} \tag{3.23}$$

Maximum unambiguous Doppler

The maximum unambiguous Doppler is analogous to the maximum unambiguous range and is given by

$$f_{D,max} = \frac{2v_{max}f_c}{c_0}. \tag{3.24}$$

The maximum unambiguous velocity is given by

$$v_{max} = \frac{c_0}{2f_c T} \tag{3.25}$$

In frequency, a large subcarrier distance alleviates the deorthogonalizing effect of a frequency offset. Therefore, it must be ensured that Δf is larger than the Doppler shift caused by the object with the maximum velocity v_{max}[52]

$$\Delta f \gg \frac{2v_{max}}{c_0} f_c \tag{3.26}$$

Doppler resolution

Along with the corresponding velocity resolution, the Doppler resolution is related to the total OFDM period and the number of symbols transmitted according to

$$\Delta v = \frac{c_0}{2MTf_c} \tag{3.27}$$

Given a maximum tolerable velocity resolution Δv_{max}, the minimum frame duration is given by

$$MT \geq \frac{c_0}{2\Delta v_{max}f_c} \tag{3.28}$$

Chapter 4

OFDM MIMO Radar System

The term multiple-input-multiple-output (MIMO) radar can be defined as a multiple-transmit-receive antenna configuration which emits independent waveforms through transmitters and these waveforms are then received by the multiple receivers [71]. In wireless communication systems the use of MIMO has been shown to have the potential of providing significantly higher capacity compared to the conventional single antenna systems [72]. When introducing multiple antennas into OFDM systems, an even better capacity performance can be achieved [73]. MIMO is an efficient technique for broadband data transmission in multipath fading environments to improve system spectral efficiency and capacity [74].

MIMO systems have led to a revolution in wireless communications [75]. Publications like [76] indicate that MIMO systems can exploit similar ideas in radar, suggesting interesting cross ideas between MIMO communications and MIMO radar.

This chapter introduces the fundamentals of MIMO concepts, the antenna configuration for MIMO radar application and the signal model for MIMO Radar systems.

4.1 MIMO Overview

MIMO techniques improve communication performance by either combating or exploiting multipath scattering in the communications channels between a transmitter and receiver. MIMO techniques combat multipath by creating what is called spatial diversity, and those techniques that exploit multipath do so by performing spatial multiplexing [77]. One of the advantages is the improvement of the data rate as well as the signal-to-noise-ratio (SNR)[53]. Some fundamental concepts are reviewed in the following sections.

4.1.1 Diversity

In most environments where wireless communication systems operate, the strength of the received signal varies with time. When the signal travel from the transmitter to the receiver in an urban environment for example, before being received the signal is reflected along multiple paths. The received signal experience phase shifts, time delays, distortion and attenuation from the environment. This effect in the signal is called fading impact and are directed related to the degradation of the communication performance by increasing the probability of

bit error [77]. An effective way to overcome such effect, is exploiting diversity in the various domains, time, space and frequency. Basically, diversity means that the same information flows through different independent paths [3].

Time Diversity

The time diversity involves transmitting the same signal at different times, separated by much more than the coherence time. In a multipath environment, this occurs naturally because the same signal arrives at the receiver by traveling over multiple physical paths, which tend to experience independent fading [3].

Frequency Diversity

The frequency diversity can be achieved by transmitting the signal on different RF frequencies that are spaced far enough that the fading occurs independently on each carrier.

Space Diversity

Space diversity refers to transmitting the same information over different physical paths between the transmitter and receiver.

4.1.2 Antenna Configuration

There are four types of antenna configuration that can be used in MIMO systems. They can be classified by the number of transmitting and receive antennas that compose the system. This section will describe the different configurations [78].

SISO

The simplest configuration is when the system operates with one antenna in the transmitter as does in the receiver. This configuration is defined as Single Input Single Output (SISO). Figure 4.1 illustrates the SISO format.
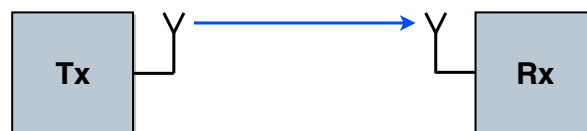
Figure 4.1: SISO configuration.

This configuration has no space diversity and no additional processing required. The advantage is simplicity. However, the interference and fading will have a stronger impact in this system.

SIMO

The Single Input Multiple Output format (SISO) it is composed by a single antenna in the transmitter and multiple antennas in the receiver as the Figure 4.2 shows.
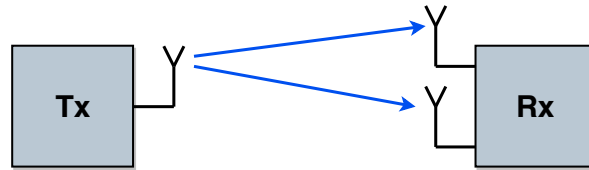
Figure 4.2: SIMO configuration.

In this configuration, it is possible to achieve receive diversity. SISO has the advantage that it is relatively easy to implement although the processing is higher in the receiver.

MISO

The Multiple Input Single Output (MISO) configuration uses multiple antennas in the transmitter and one antenna in the receiver as illustrated in Figure 4.3.
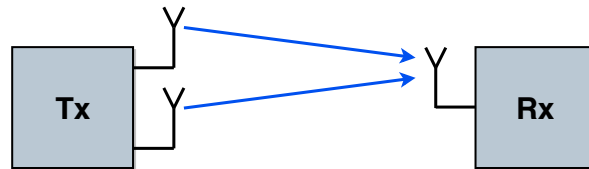
Figure 4.3: MISO configuration.

In this configuration, the diversity is achieved by the transmitter and the processing is higher on the transmitter side.

MIMO

Lastly, the Multiple Input Multiple Output (MIMO) is composed by multiple antennas in the transmitter and multiple antennas in the receiver. This configuration allows the transmission of multiple data streams simultaneously in frequency and time. In order to be able to separate the data from the different paths it is necessary to utilize coding on the spatial channels. This requires higher processing but provides additional channel robustness and high spectral efficiency. Figure 4.4 represents the MIMO configuration.
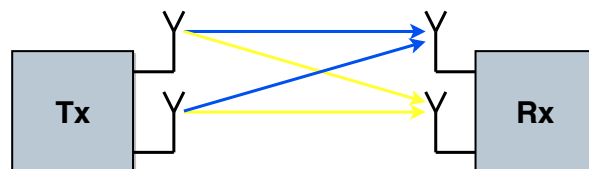
Figure 4.4: MIMO configuration.

4.1.3 Receive Diversity

Consider multiple antennas at the receiver and a single antenna at the transmitter. The extraction and combining of the received transmitted signal replicas is called receive diversity.

Figure 4.5 illustrates a scenario of receive diversity.
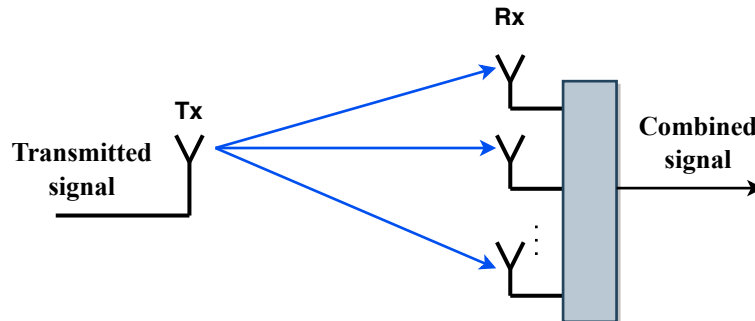
Figure 4.5: Communication system with receive diversity.

Consider the receive antenna elements spaced far enough, to make the channels independent. The receiver is able to reduce the effect of fading by combining multiple independent fading signals [77]. Receive diversity can achieve both diversity and antenna gain. The diversity gain is related to the fact that the channels are independent. The antenna gain is related to the fact that the noise terms added at each receiver are independent [3].

Some of the schemes that combine the multiple replicas are summarized as [3],

- **Maximal Ratio Combining (MRC):** All paths are co-phased and summed with optimal weighting to maximize combiner output SNR. This scheme is also known as matched filter (MF).

- **Equal Gain Combining (EGC):** The signal is co-phased on each branch and then combined with equal weight. The complexity reduction by means of equal gains, makes the performance of EGC lower compared to the MRC, presenting a lower antenna gain.

- **Selection Combining (SC):** The selection algorithm compares the instantaneous amplitude of each channel and chooses the branch with the largest amplitude.

4.1.4 Transmit Diversity

The main idea of transmit diversity is to provide a diversity or coding gain by sending redundant signals over multiple transmit antennas [77]. To achieve transmit diversity, multiple antennas are only required at the transmitter.

To achieve coherent detection at the receiver, before transmission the signal is precoded. Figure 4.6 shows the basic principle of transmit diversity.
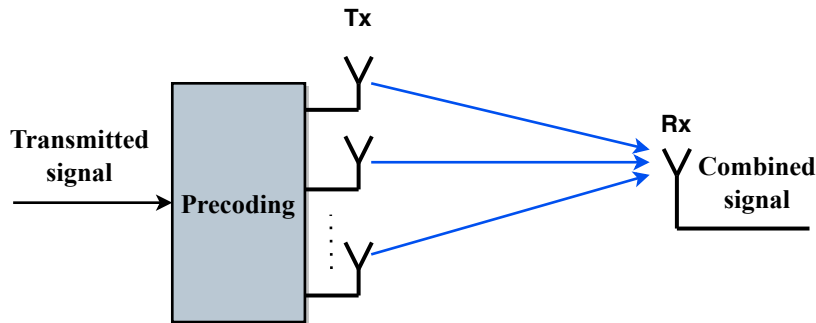
Figure 4.6: Communication system with transmit diversity.

The two main types to achieve transmit diversity are closed loop transmit diversity and open loop transmit diversity [3].

Closed Loop technique

Closed loop technique requires channel information to assist the transmitter in choosing a transmit format over the multiple transmit antennas [79].

There are two ways to provide information about the channel. One way is to acquire the information in the uplink by the base station. The other way is to allocate a feedback channel with channel information.

Open Loop technique

The open loop technique does not require knowledge of the channel In open loop transmit diversity space-time/frequency codification is used.The most common space-time/frequency codes are Space-Time Trellis Code (STTC) and space time/frequency block coding (STBC or SFBC). STTC provides both coding and diversity gains but requires more complexity [3]. In this work we study the block coding with an adoption of the Alamouti scheme.

The Alamouti scheme was first proposed in [80] which, consider a system composed by two transmit antennas. The bits are modulated and then converted into symbols, s_1 and s_2. In this scheme the symbols s_1 and s_2 are transmitted simultaneously, from the two Tx antennas in the first symbol period. In the next symbol period the two Tx antennas transmits $-s_2^*$ and s_1^*, where, $*$ represents the complex conjugate. Table 4.1 represents the transmission code. The transmitted signal matrix can be written as

$$\mathbf{S} = \begin{bmatrix} s_1 & -s_2^* \\ s_2 & s_1^* \end{bmatrix} \qquad (4.1)$$

Time	Ant1	Ant2
t	s_1	s_2
t+T	$-s_2^*$	s_1^*

Table 4.1: Alamouti encoder scheme [3].

37

Figure 4.7 illustrates the Alamouti block diagram.
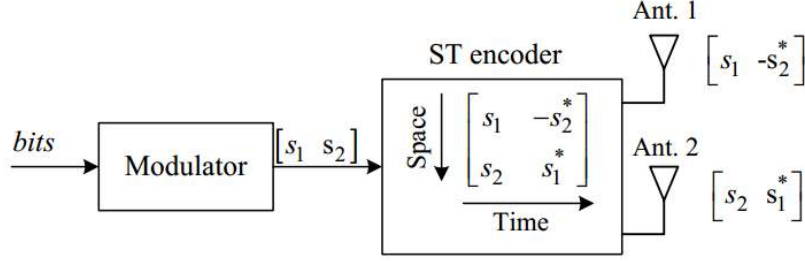
Figure 4.7: Alamouti scheme with 2 transmit antennas [3].

The channel for antenna 1 is h_1 and for the antenna 2 is h_2, and is assumed to remain constant for a duration of two symbols across the two transmit antennas. Figure 4.8 shows the Alamouti decoder scheme.
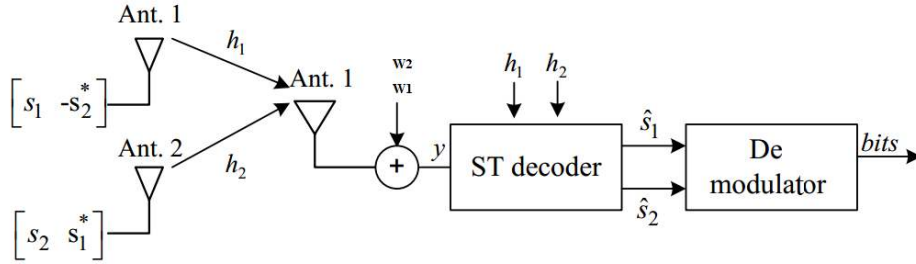
Figure 4.8: Alamouti scheme with 1 receive antenna [3].

Being T the symbol duration and assuming the channels between two adjacent instants, are highly correlated then the received signal r_1 and r_2 at time t and $t + T$ is given by [80]:

$$r_1 = r(t) = h_1 s_1 + h_2 s_2 + w_1 \tag{4.2}$$

$$r_2 = r(t + T) = -h_1 s_2^* + h_2 s_1^* + w_2 \tag{4.3}$$

The previous equation can be written in matrix form as

$$\begin{bmatrix} r_1 & r_2 \end{bmatrix} = \begin{bmatrix} h_1 & h_2 \end{bmatrix} \begin{bmatrix} s_1 & -s_2^* \\ s_2 & s_1^* \end{bmatrix} + \begin{bmatrix} w_1 & w_2 \end{bmatrix} \tag{4.4}$$

The equation (5.22) can be rewritten as

$$\begin{bmatrix} r_1 \\ r_2^* \end{bmatrix} = \begin{bmatrix} h_1 & h_2 \\ h_2^* & -h_1^* \end{bmatrix} \begin{bmatrix} s_1 \\ s_2 \end{bmatrix} + \begin{bmatrix} w_1 \\ w_2^* \end{bmatrix} \tag{4.5}$$

The receiver combines the signals as follows

$$\tilde{s}_1 = h_1^* r_1 + h_2 r_2^* \tag{4.6}$$

$$\tilde{s}_2 = h_2^* r_1 - h_1 r_2^* \tag{4.7}$$

The detected symbols can be written as

$$\tilde{s}_1 = \|h\|^2 s_1 + h_1^* w_1 + h_2 w_2^* \tag{4.8}$$

$$\tilde{s}_2 = \|h\|^2 s_2 - h_1 w_1^* + h_2^* w_1 \tag{4.9}$$

Where, $\|h\|^2$ represents the vector norm of the channel given by $|h_1|^2 + |h_2|^2$.

4.1.5 Spatial Multiplexing

SISO and MISO systems provide diversity and antenna gains but no multiplexing gain (also called degree-of-freedom) [3]. Spatial multiplexing combines multiple data streams and transmits them in parallel at the same frequency and time slot over the MIMO multipath channel.

In spatial multiplexing, multiple signals are assigned to different spatial channels over the same frequency band, instead of time or frequency slots, and as a result the system capacity increases without bandwidth expansion [77]. Figure 4.9 shows a block diagram of a spatial multiplexing MIMO system. There three main components represented are the precoder, postcoder and the communications channel itself. The precoder maps the multiple input data streams, that will be transmitted, to the multiple transmit antennas. The postcoder, processes the signals from the multiple antennas and generates estimates of the data streams. Lastly, the channel must have a significant amount of multipath scattering. A MIMO system using spatial multiplexing can increase the transmission rate by a factor of $min(P, Q)$, where P represents the number of transmit antennas and Q the number of receive antennas.
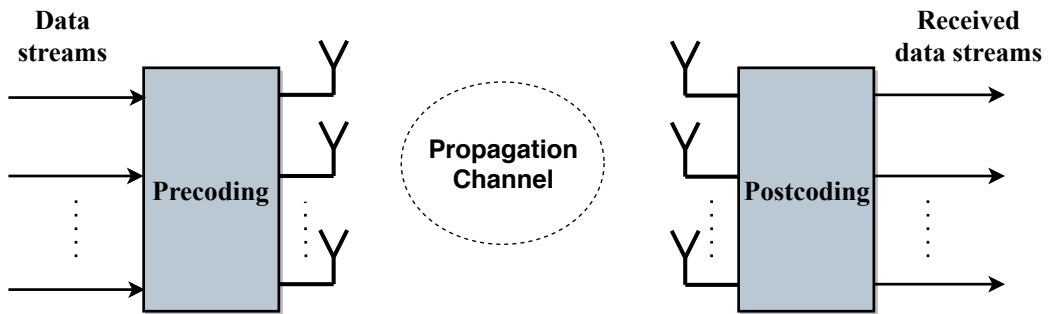
Figure 4.9: MIMO communication system using spatial multiplexing.

4.2 Antenna Configuration for MIMO Radar

Based on the antenna configuration the MIMO Radar can be classified as widely separated or colocated. With widely separated antennas the MIMO radar has the ability to improve radar performance by exploiting RCS diversity, since the target appears to be spatially distributed, providing different RCS at each antenna element [81],[50]. The definitions presented early in section (4.1.3) for MIMO communication can be applied as well to MIMO

radar. The fact that we obtain independent information about the target and combine it at the receiver warrant a high-resolution for target information. In colocated MIMO radar, the RCS observed by each antenna element is indistinguishable [50]. The target is assumed to be in the far-field scenario and modeled as a point.

An antenna array is a configuration of multiple antenna elements arranged and interconnected in space to obtain a directional radiation pattern [82]. The antenna arrays can be constructed in various types of geometric configurations. A linear array is the most elementary form in which the centers of the elements of the array are aligned along a straight line [82].

In this work, it is studied the colocated MIMO radar with a uniform linear antenna array. In this section, we briefly discuss the virtual array concept and the basics of angle estimation.

4.2.1 Virtual Array Concept

A virtual array is a technique where the number of receiver antennas becomes more than the physical number of antennas through a specific individual position of each antenna into the antenna array, and by means of signal processing. The positions are the convolution of the original transmit and receive array elements [41],[83].

Consider a MIMO radar system composed by a transmitter with a uniform linear antenna array with P elements, and a receiver with a uniform linear antenna with Q elements. A single path from a transmit antenna to the target and back to an Rx antenna is called a spatial channel. The number of spatial channels represents the virtual antennas and can be express by the product $P \times Q$ that gives us the number of the virtual antenna elements. Consider the same number of physical antennas (total number of transmit and receive antennas) for a SISO system and for a MIMO system, then the number of spatial channels for the MIMO systems is larger than a system utilizing the SISO configuration. For a $P \times QM$ MIMO Radar the spatial channels can be arranged into an equivalent array consisting of a single Tx and $P \times Q$ Rx antennas, which is denominated virtual array. In the following two different scenarios are considered to exemplify the virtual array concept.

In the first scenario, as Figure 4.10 shows, the antenna elements are separated by a distance of $d_{ant} = \lambda/2$ both in the transmit and receive antenna array. This figure also shows the correspondent virtual antenna array. The correspondent virtual array, which is constructed by calculating the convolution from both transmit and receive antenna elements of the real array antenna positions, each one with a correspondent phase, is over-represented [84]. In this example, we have repetitive elements with the same phase rotation resulting only in five unique responses and four repeated terms.
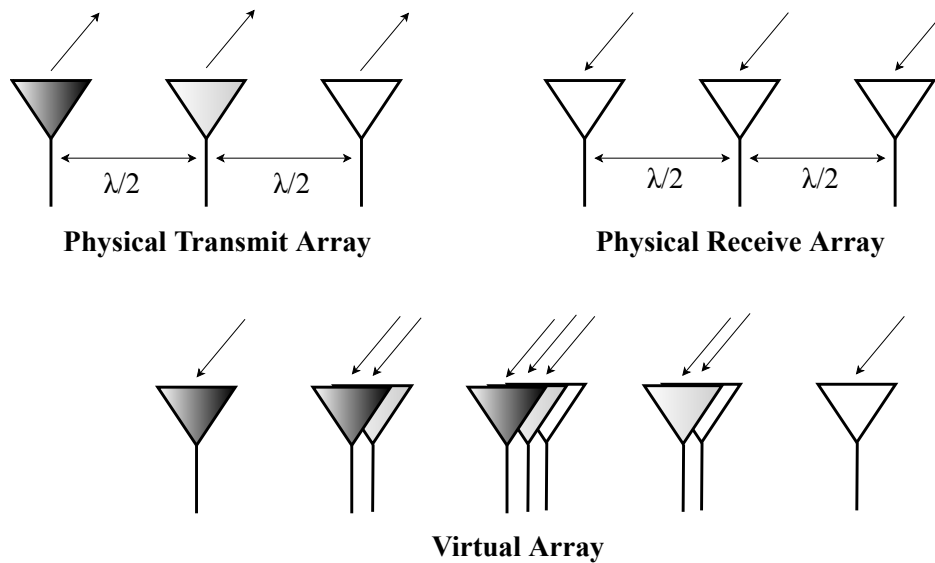
Figure 4.10: MIMO radar system with the corresponding virtual array.

In order to achieve the maximum number of non repetitive Rx signals, the physical transmit and receive linear array elements must be arranged to result in a maximum unique response. Figure 4.11 illustrates a scenario of a Uniform Linear Virtual Array (ULVA), where the distance of each transmit antenna element is $Q \times \lambda/2$ and the distance of each receive antenna element is $\lambda/2$. The resulting receive virtual array is composed by $P \times Q$ elements.
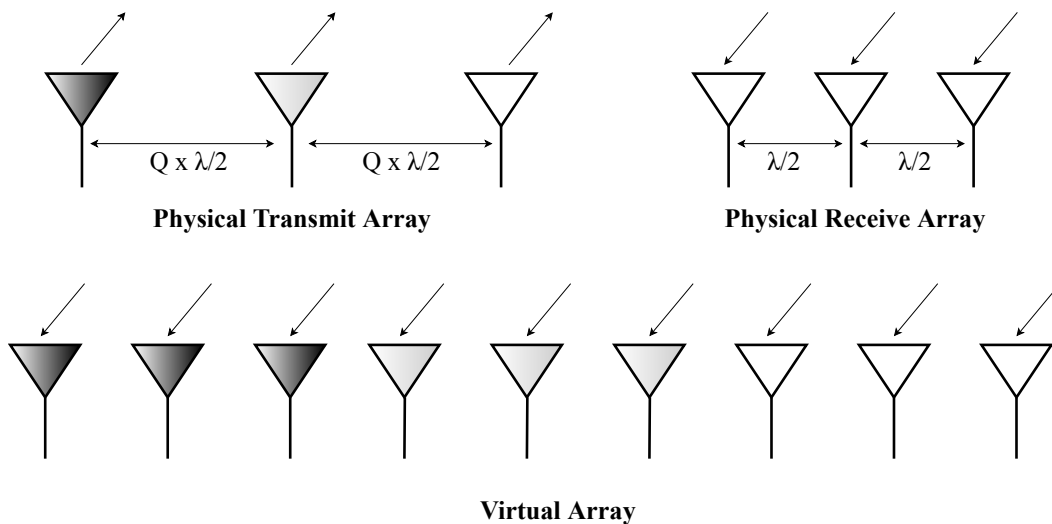
Figure 4.11: A ULA MIMO radar system with the corresponding virtual array.

4.2.2 Angle estimation basics

While the velocity and the range estimation, are influenced by the signal model parameters the angular estimation is influenced by the antenna array configuration. Let us start with the

simplest case to estimate the angle. In order to obtain information about the angle it requires at least two receive antennas (Rx). Figure 4.12 show the scenario of one transmit antenna (Tx) and two receivers antennas. The two Rx antennas are separated by a distance d_{ant}.
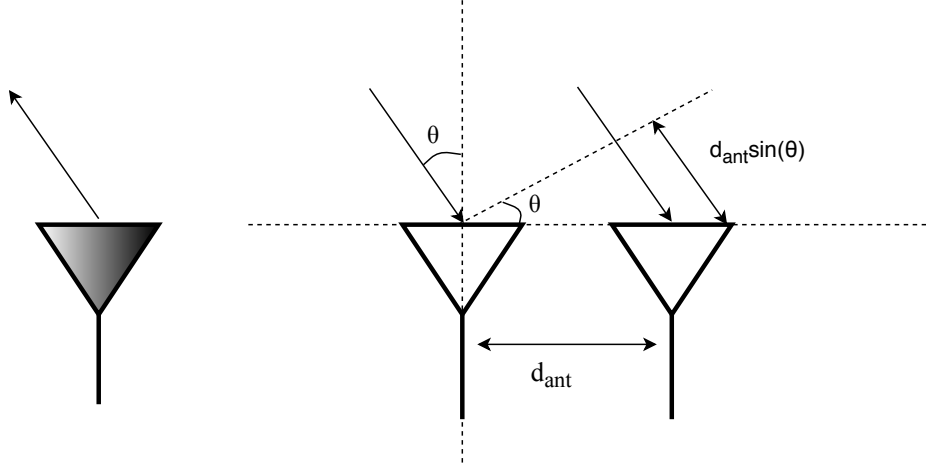
Figure 4.12: Angle estimation.

Consider a transmitted signal from the Tx antenna that hits an object. The signal reflected from the object will be received by both Rx antennas with an angle (Θ). The signal reflected from the object will travel an additional distance of $d_{ant}sin(\Theta)$ to reach the second antenna Rx. This additional travel will cause a phase difference of w in the second Rx antenna regarding to the first Rx antenna, given by

$$w = \frac{2\pi}{\lambda} d_{ant} \sin\left(\Theta\right).$$ (4.10)

Therefore, the angle can be estimated by computing from the previous equation,

$$\Theta = \arcsin\left(\frac{w\lambda}{2\pi d_{ant}}\right).$$ (4.11)

The phase difference, w, will lead to angle (Θ) in the range $(-90°, 90°)$.

Angle Resolution

The angular resolution is the minimum separation of two closely targets for the radar to perform angle estimation correctly. It is expressed as

$$\Delta\Theta = \frac{\lambda}{PQd_{ant}}$$ (4.12)

4.3 OFDM MIMO Radar Signal Model

With the insertion of multiple antennas in the radar system, the OFDM subcarriers must be assigned to the antennas in such a way that they are all orthogonal to each other. In

order to create a set of orthogonal transmit signals, the OFDM signal structure has some modifications [41]. Figure 4.13 shows an example of how the subcarriers are assignment along the transmit antenna array elements, in this case, composed by $P = 3$ elements. The total number of subcarriers (N) is distributed among the different antennas.
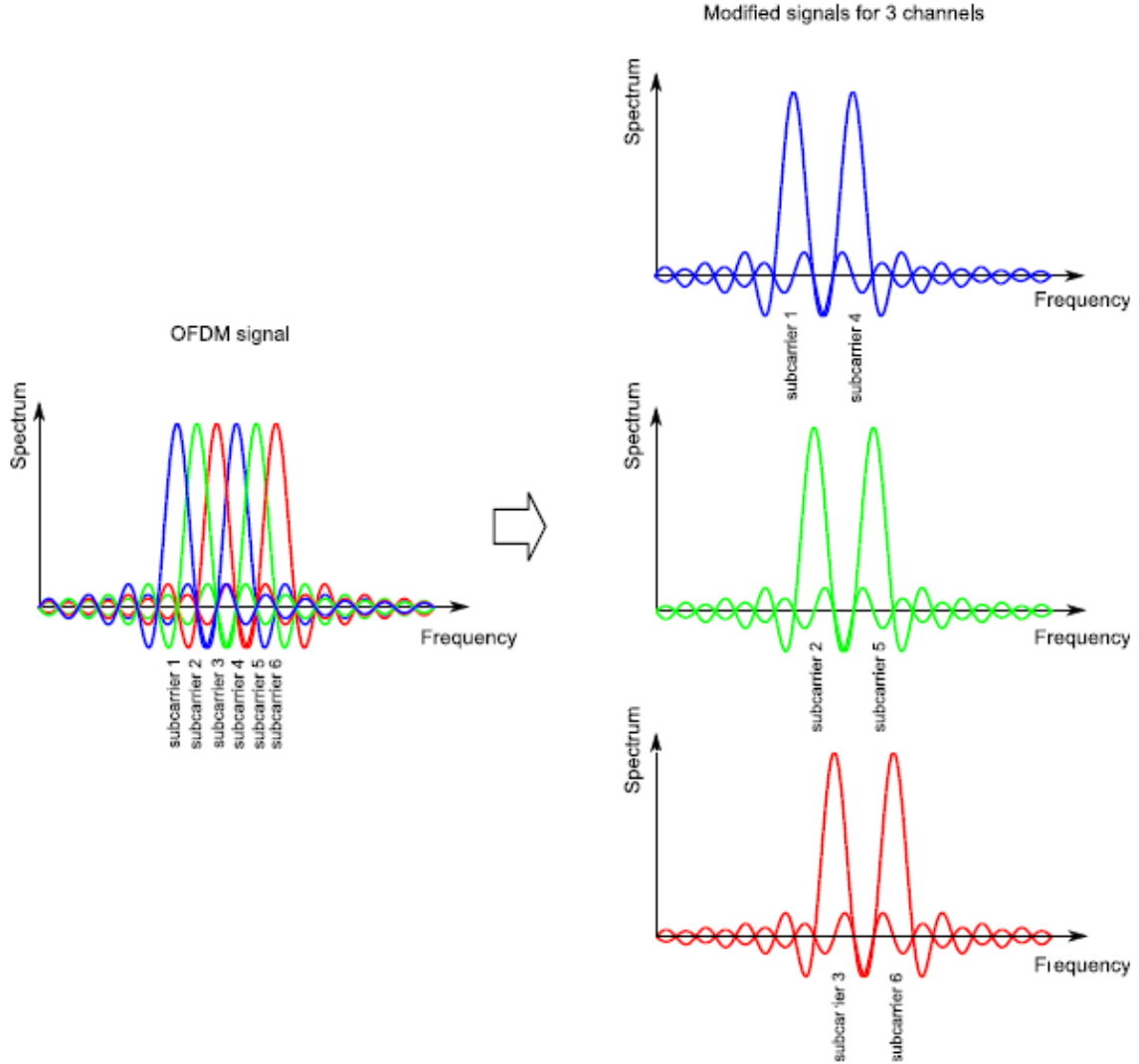
Figure 4.13: Subcarriers distribution along the transmit antennas [85].

Consider that each modulation symbol $c_{k,l}$ is organized into the matrix $\mathbf{F}_{Tx}$ as

$$\mathbf{F}_{Tx} = \begin{bmatrix} c_{0,0} & \cdots & c_{0,N-1} \\ \vdots & \ddots & \vdots \\ c_{N-1,0} & \cdots & c_{N-1,M-1} \end{bmatrix} \tag{4.13}$$

$\mathbf{F}_{Tx} \in \mathbb{C}^{N \times M}$ describes the complete OFDM frame carrying the modulated payload and $\mathbf{F}_{Tx}(k,l) \in \mathcal{A}$ the modulation symbol, where $\mathcal{A}$ is the modulation alphabet, in this work we

43

use BPSK.

Consider a radar equipped with $P \times Q$ transmit(Tx) and receive(Rx) antennas. $\mathbf{F}_{Tx}$ is split in P parts $\mathbf{F}_{Tx,p}$, thereby every k_p-th subcarrier is allocated to p-th Tx antenna, with $0 \leq p \leq P-1$, $k_p = p+i \cdot P$ and $0 \leq i \leq N/P-1$ as proposed in [86]. The variable i represents the subindex of the subcarrier allocated to one Tx antenna and k_p the index addressing these subcarriers in the complete frame.

The transmit signal of each p-th antenna can be described as

$$s_p(t) = \sum_{l=0}^{M-1} \sum_{i=0}^{N-1} \mathbf{F}_{Tx,p}(k,l) \cdot e^{j2\pi k_p \Delta f t} \cdot rect\left(\frac{t - lT}{T}\right), \tag{4.14}$$

with,

$$\mathbf{F}_{Tx,p}(k,l) = \begin{cases} \mathbf{F}_{Tx}(k,l), & \text{if } k = p + i \cdot P, \ 0 \leq i \leq N/P - 1 \\ 0, & \text{otherwise} \end{cases} \tag{4.15}$$

Each q-th receiver antenna, receives the signals of all transmit antennas and can reconstruct the complete payload data frame. Take in count the delay and the frequency shift during the propagation and the performance of a fast Fourier transform over each OFDM symbol on the receiver side. The OFDM frame at q-th receiver antenna can be written in the frequency domain as

$$\mathbf{F}_{Rx,q}(k,l) = \sum_{p=0}^{P-1} \mathbf{F}_{Tx,p}(k,l) \cdot \sum_{h=0}^{H-1} b_h \cdot e^{-j2\pi k \Delta f \tau_{p,q,h}} \cdot e^{j2\pi f_{D,p,q,h} lT} + \mathbf{W}_q(k,l). \tag{4.16}$$

In relation to the receivers(Rx), each one receives the interleaved signals of all Tx antennas to reconstruct the complete data frame. $\tau_{p,q,h}$ is the round-trip distance from p-th Tx antenna to the target and back to the q-th Rx antenna. $f_{D,p,q,h}$ is given by: $f_{D,p,q,h} = \frac{2v_{rel,p,q,h}f_c}{c_0}$.

Chapter 5

OFDM MIMO RadCom System

The demand for radio-frequency bandwidth is rising, with the growing number of users and applications [87]. The radar and communication systems are two of main players in this regard and are central to make the IoT paradigm a reality. The separation of the radar and communication system is a waste of resources and the interference between the two systems is inevitable. On the other hand, their integration on a single hardware, enables the paradigm of dual functionality devices with communication and radar sensing capabilities fundamental to cope with the challenges of future IoT. A joint radar and communication system has significant advantages in terms of cost, size, performance and spectrum usage, as by working collaboratively the interference of each system on the other can be reduced and the spectrum efficiency of the whole system can be promoted [88].

In this work, the integration of radar and communication systems is accomplished by using OFDM as a common waveform and the use of Alamouti coding enables both the achievement of spatial diversity, for the communication functionality, and of transmit signal orthogonality required to improve resolution, for the radar functionality. The evaluation of the previous method as a way to achieve radar and communication integration was accomplished by developing a simulation platform, first only with the radar functionality, for SISO and MIMO configurations, and then with both radar and communication functionalities.

This chapter is divided into three parts. The first part, deals with the OFDM MIMO Radar system comprising the system model without communication, the antenna architecture and the radar imaging. The second part deals with the inclusion of the communication in the MIMO Radar system comprising the signal-sharing technique used to recovery the payload data and maintain the radar functionality, presenting the features of the radar terminal and the communication terminal designed. Lastly, the performance results are presented.

5.1   OFDM MIMO Radar System Developed

In a first approach it is assumed a monostatic radar with a single transmitter, single receiver where it is only possible to obtain information about the range of the target and the Doppler shift. It is also considered that there are no other signal sources during transmission and the only signal received is the transmitted signal after hitting the targets. The only distortion considerate is the additive white Gaussian noise (AWGN). In section 5.2, the system

will expand to a MIMO Radar system to obtain an estimate of each target angle.

5.1.1 System model

Consider a monostatic radar with a single transmiting and a single receiving antenna. Figure 5.1 illustrate such radar system. The system implemented starts by transmitting the OFDM signal $s(t)$, the signal will hit a total number, H, of objects and the received signal, $r(t)$, is the superposition of reflections of the original signal.
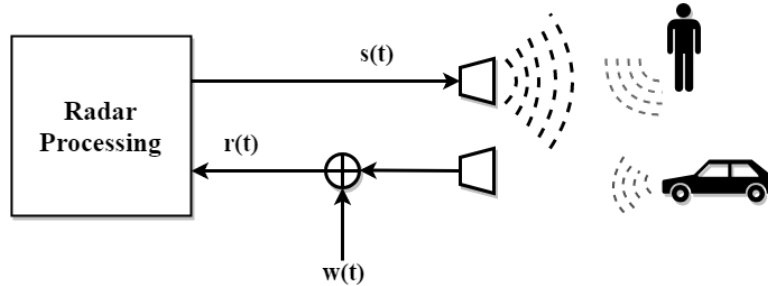
Figure 5.1: Radar System schematic.

Consider that the complex symbols $c_{k,l}$ are modulated using BPSK and are organized in the matrix $\mathbf{F}_{Tx}$ according to

$$\mathbf{F}_{Tx} = \begin{bmatrix} c_{0,0} & \cdots & c_{0,N-1} \\ \vdots & \ddots & \vdots \\ c_{N-1,0} & \cdots & c_{N-1,M-1} \end{bmatrix} \in \mathcal{A}^{N \times M}. \tag{5.1}$$

Every row represents a subcarrier and every column represents an OFDM symbol of $\mathbf{F}_{Tx}$. In case a subcarrier is left empty each element $c_{k,l}$ correspondent is set to zero.

Starting from the equation (3.19) present in section (3.2) and assuming the matrix notation, the received frame matrix $\mathbf{F}_{Rx}$ is given by

$$\mathbf{F}_{Rx}(k,l) = \sum_{h=0}^{H-1} b_h \mathbf{F}_{Tx}(k,l) \cdot \mathrm{e}^{j2\pi f_{D,h}lT} \mathrm{e}^{-j2\pi \tau_h \Delta fk} + \widetilde{\mathbf{W}}(k,l), \tag{5.2}$$

where τ_h the delay and $f_{D,h}$ the Doppler shift.

The frequency shift $f_{D,h}$, corresponds to a modulation of every row of F_{Tx} with a discretely sampled complex sinusoid $\mathrm{e}^{j2\pi T f_{D,h}l}$, $l = 0 \ldots M-1$. The delay causes a phase shift of every symbol $c_{k,l}$ given by $\mathrm{e}^{-j2\pi \Delta fk}$, where k is the index of the sub-carrier, $k = 0 \ldots N-1$. $\widetilde{\mathbf{W}}(k,l) \in \mathcal{A}^{N \times M}$ is the matrix representation of the AWGN. Its elements are complex Gaussian distributed with zero-mean and variance γ^2.

The received matrix ($\mathbf{F}_{Rx}$) contains the matrix $\mathbf{F}_{Tx}$ that has no purpose for the parameters that we want to estimate. The parameters we have interest are the τ and f_D. Therefore, the

next step is to perform an element-wise division of (5.2) by $\mathbf{F}_{Tx}(k.l)$ to obtain,

$$\mathbf{F}(k,l) = \frac{\mathbf{F}_{Rx}}{\mathbf{F}_{Tx}} = \sum_{h=0}^{H-1} b_h \cdot e^{j2\pi f_{D,h}lT} e^{-j2\pi\tau_h\Delta fk} + \frac{\widetilde{\mathbf{W}}(k,l)}{\mathbf{F}_{Tx}(k,l)}. \tag{5.3}$$

The $\mathbf{F}(k,l)$ matrix represents the matrix transfer function that will be used for the radar processing to obtain the radar imaging.

5.1.2 Radar Processing

The periodogram is used as a part of the radar processing to develop the radar imaging. This section explains the periodogram concept and the adaptation for our case scenario.

Periodogram for Range and Velocity estimation

Periodogram is used to identify sinusoids in a discrete-time signal [64]. For a periodogram with one-dimension, where $s(k)$ of length N samples is the discrete-time signal, the periodogram is obtained from

$$Per_{s(k)}(f) = \frac{1}{N}\left|\sum_{k=0}^{N-1} s(k)e^{-j2\pi fk}\right|^2. \tag{5.4}$$

In digital systems, the common way to calculate this is to quantize the frequency in regular intervals and use the Fast Fourier Transformation(FFT) [64],

$$Per_{s(k)}(n) = \frac{1}{N}\left|\sum_{k=0}^{N-1} s(k)e^{-j2\pi\frac{nk}{N_{Per}}}\right|^2. \tag{5.5}$$

$$= \frac{1}{N}\left|FFT_{N_{Per}}[s(k)]\right|^2. \tag{5.6}$$

where, normally N_{Per} takes a value higher than N.

In our case we need a two dimension periodogram, to use as input the matrix $\mathbf{F}$. For the two dimensional case the periodogram is obtained from [89]

$$Per_F(n,m) = \frac{1}{NM}\left|\underbrace{\sum_{k=0}^{N_{Per}-1}\left(\overbrace{\sum_{l=0}^{M_{per}-1}(F)_{k,l}e^{-j2\pi\frac{lm}{M_{Per}}}}^{N\,FFTs\,of\,length\,M_{Per}}\right)e^{j2\pi\frac{kn}{N_{Per}}}}_{M_{Per}\,IFFTs\,of\,length\,N_{Per}}\right|^2. \tag{5.7}$$

A possible choice for M_{Per} and N_{Per} is $M_{Per} = 8 \times M$ and $N_{Per} = 8 \times N$.

Accordingly to (5.14) to obtain the 2D periodogram first, the columns and rows of matrix $\mathbf{F}$ are zero-padded, then every row is processed with a FFT and, every columns with an IFFT. The final matrix has a dimension of $N_{Per} \times M_{Per}$.

To adapt the periodogram to the radar case, the indices n and m must be translated as

$$d = \frac{nc_0}{2\Delta f N_{Per}}, \; n = 0, \dots, N_{Per} - 1; \tag{5.8}$$

$$v = \frac{mc_0}{2f_C T_0 M_{Per}}, \; m = \frac{-M_{Per}}{2}, \dots, \frac{M_{Per}}{2} - 1. \tag{5.9}$$

5.2 MIMO Radar System Developed

MIMO radar system employs multiple transmitters, multiple receivers, and multiple waveforms to exploit all available degrees of freedom [90]. As we refer in the previous section a system with single transmitter single receiver is only able to perform range and velocity estimation. In this section the MIMO system is introduced to propose a capable form to estimate angle information.

5.2.1 System model

Accordingly to the description provided in section 4.3, the OFDM frame at the Rx antenna q can be written in the frequency domain as (see (4.16))

$$\mathbf{F}_{Rx,q}(k,l) = \sum_{p=0}^{P-1} \mathbf{F}_{Tx,p}(k,l) \cdot \sum_{h=0}^{H-1} b_h \cdot \mathrm{e}^{-j2\pi k\Delta f\tau_{p,q,h}} \cdot \mathrm{e}^{j2\pi f_{D,p,q,h}lT} + \mathbf{Z}_q(k,l). \tag{5.10}$$

In relation to the receivers (Rx), each one receives the interleaved signals of all Tx antennas to reconstruct the complete data frame. H is the number of targets, b_h is the attenuation factor. $\tau_{p,q,h}$ is the round-trip distance from p-th to the target and back to the q-th antenna. $f_{D,p,q,h}$ is given by: $f_{D,p,q,h} = \frac{2v_{rel,p,q,h}f_c}{c_0}$.

Consider a system equipped with $P \times Q$ antennas adopting the virtual antenna concept the equivalent of the previous MIMO system is a system with a $1 \times P \cdot Q$ configuration, where the receiving antennas are separated by a distance $\lambda/2$. Just like in OFDM Radar we perform a element-wise division to the equation (5.10) in order to remove from the equation the transmitted OFDM frame.

$$\mathbf{F}_q(k,l) = \frac{\mathbf{F}_{Rx,q}(k,l)}{\mathbf{F}_{Tx}(k,l)} = \sum_{h=0}^{H-1} b_h \cdot \mathrm{e}^{-j2\pi k\Delta f\tau_{q,h}} \cdot \mathrm{e}^{j2\pi f_{D,q,h}lT} + \frac{\widetilde{\mathbf{W}}_q(k,l)}{\mathbf{F}_{Tx}(k,l)}. \tag{5.11}$$

The delay can be expressed as $\tau_{q,h} = \tau_h + \tau_{ant}$. τ_h represents the round-trip time from the Tx antennas to the first Rx antenna of the virtual array, and the τ_{ant} the additional distance from the first Rx antenna to the q-th Rx antenna. The τ_h term is given by

$$\tau_h = 2\frac{d_h}{c_0}, \tag{5.12}$$

and τ_{ant} by

$$\tau_{ant} = (q-1)\frac{\lambda}{2}\frac{\sin(\Theta_h)}{c_0}, \tag{5.13}$$

5.2.2 Radar Processing

In this section we explain how to estimate the three parameters(range, velocity and angle) of a target.

Consider the matrix $\mathbf{F}_q(k,l)$ given by (5.11), where q-th is the index of the virtual antenna array. The matrix represents the radar channel with range and Doppler information for the virtual receive antenna q. The range is estimated with an inverse fast Fourier transform (IFFT) along the columns and the Doppler is estimated with a fast Fourier transform (FFT) along the rows of $\mathbf{F}_q(k,l)$ to obtain matrix $\mathbf{G}_q(k,l)$

$$
G_q(k,l) = \sum_{k=0}^{N-1} \overbrace{\left(\underbrace{\sum_{l=0}^{M-1} \mathbf{F}_q(k,l) e^{-j2\pi \frac{lm}{M}}}_{M\ IFFTs\ of\ length\ N} \right)}^{N\ FFTs\ of\ length\ M} e^{j2\pi \frac{kn}{N}} . \tag{5.14}
$$

$$
\mathbf{G}(k,l) = \begin{bmatrix} G_1(k,l) \\ G_2(k,l) \\ G_3(k,l) \\ \vdots \\ G_Q(k,l) \end{bmatrix} , \tag{5.15}
$$

and a matrix $B(\Theta)$ of size $\mathbb{C}^{Q \times 1}$,

$$
B(\Theta) = \begin{bmatrix} 1 \\ e^{-j2\pi(\sin\Theta d_{ant}/\lambda)} \\ \vdots \\ e^{-j2\pi(\sin\Theta(Q-1)d_{ant}/\lambda)} \end{bmatrix} . \tag{5.16}
$$

d_{ant} is the space between the Rx antenna elements and Θ range between $-90°$ and $90°$. The resulting matrix can be expressed as

$$
H(k,l,\Theta) = \langle G(k,l), B(\Theta) \rangle. \tag{5.17}
$$

5.3 RadCom System

At this point, we are able to obtain a radar imaging. In this section, we intend to accomplish the radar and communication system integration and present a design of a joint Radar Communication system (RadCom System). The integration of the two subsystems is not just at the hardware level. In this case the signal processing used in the radar system will have a double functionality. The radar should be able to add communication function while maintaining the original radar function, sharing the same waveform design [91].

5.3.1 System model

Figure 5.2 illustrates the scenario implemented in this work. The RadCom signal is transmitted from the RadCom system. The signal transports communication information to the mobile device equipped with a receiving antenna. At the same time, the signal is reflected from the target in the area. The RadCom system receives the echoes of it is own transmit signal and detects the presence of reflecting objects. For communication processing, the modulation type is perfectly known to the communication terminal. For radar processing, the transmitted signal is known at the radar receiver.

Before the transmission the data is encoded by using the Alamouti coding to allow joint radar and communications functionalities.
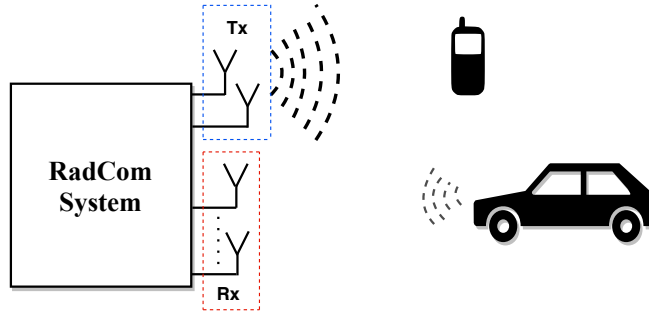
Figure 5.2: RadCom System scenario.

RadCom Transmitter

Consider a RadCom system with 2 Tx antennas. Considering the Alamouti space-time scheme in OFDM systems, Figure 5.3 shows the block diagram of the RadCom Transmitter implemented.
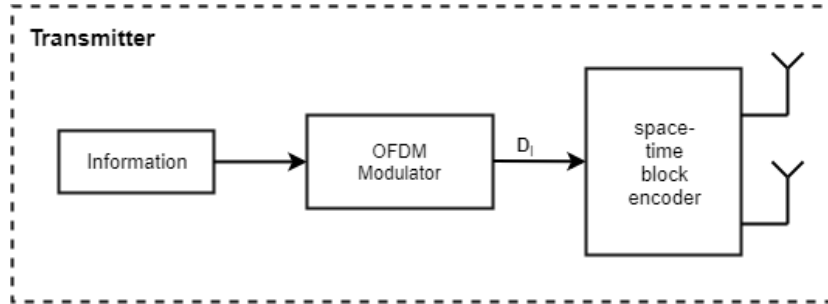
Figure 5.3: Block diagram of the RadCom Transmitter.

The binary data stream is first modulated and mapped from a BPSK modulation alphabet to a sequence of symbols $D_l[k]$ given by

$$\mathbf{D}_l[k] = \Big[D_l[0], D_l[1], ..., D_l[N-1] \Big]^T \tag{5.18}$$

where l is the OFDM symbol index ($l = 0, ..., M-1$) and N the total number of subcarriers.

Then a STBC operation is performed over $D_l[k]$ and it is turned into two parallel information vectors according to Table 5.1.

OFDM Block	Ant1	Ant2
n	$s_1[n]$	$s_2[n]$
$n+1$	$s_1[n+1] = -s_2^*[n]$	$s_2[n+1] = s_1^*[n]$

Table 5.1: Alamouti code[92].

The output vectors during two consecutive transmission periods(n and $n+1$) are given by,

$$
\begin{aligned}
s_1[n,k] &= [D_l[0], D_l[1], \cdots, D_l[k]], \\
s_2[n,k] &= [D_l[k+1], D_l[k+2], \cdots, D_l[2k]], \\
s_1[n+1,k] &= [-D_l^*[k+1], -D_l^*[k+2], \cdots, -D_l^*[2k]], \\
s_2[n+1,k] &= [D_l^*[0], D_l^*[1], \cdots, D_l^*[k]].
\end{aligned}
\tag{5.19}
$$

On each serial data stream an IFFT is performed and a cyclic prefix (CP) is added to output samples.

Communication terminal

Consider a communication terminal with one Rx antenna at a different place from the RadCom system. We pretend to recover the payload data sent from the RadCom system. Figure 5.4 illustrates the scheme of the Communication terminal implemented.
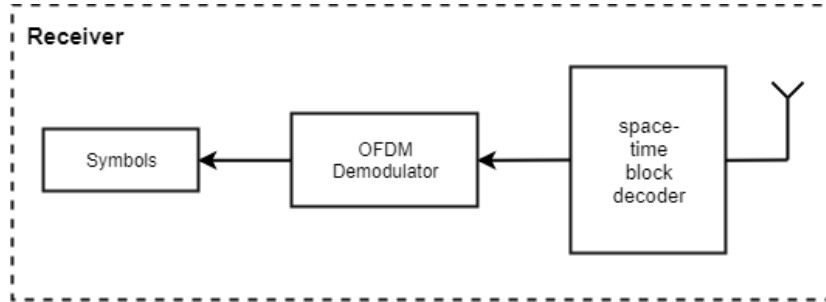
Figure 5.4: Alamouti scheme with 1 receive antenna.

Assuming the channel to be static over two OFDM blocks, where H_i represents the channel from i-th transmit antenna to the receive antenna. Removing the cyclic prefix and making the FFT operation, the received signals at the k-th subcarrier are given by[93]:

$$
r[n,k] = \sum_{i=1}^{2} H_i[k]s_i[n,k] + z[n,k]
\tag{5.20}
$$

$$
r[n+1,k] = \sum_{i=1}^{2} H_i[k]s_i[n+1,k] + z[n+1,k].
\tag{5.21}
$$

We can rewrite the equation (5.20) and (5.21) in matrix form as

$$\begin{bmatrix} r[n,k] \\ r[n+1,k] \end{bmatrix} = \begin{bmatrix} s_1[n,k] & s_2[n,k] \\ s_1[n+1,k] & s_2[n+1,k] \end{bmatrix} \begin{bmatrix} H_1[k] \\ H_2[k] \end{bmatrix} + \begin{bmatrix} w_1 \\ w_2 \end{bmatrix} \tag{5.22}$$

The matrix equation (5.22) can be transformed into

$$\begin{bmatrix} r[n,k] \\ r^*[n+1,k] \end{bmatrix} = \begin{bmatrix} H_1[k] & H_2[k] \\ H_2^*[k] & -H_1^*[k] \end{bmatrix} \begin{bmatrix} S_1[n,k] \\ S_2[n,k] \end{bmatrix} + \begin{bmatrix} w_1 \\ w_2 \end{bmatrix} \tag{5.23}$$

The outputs are sent to the STBC decoder and the two parallel information streams sent are estimated

$$\tilde{s}_1[n,k] = \hat{H}_1^*[k]r[n,k] + \hat{H}_2[k]r^*[n+1,k] \tag{5.24}$$

$$\tilde{s}_2[n,k] = \hat{H}_2^*[k]r[n,k] - \hat{H}_1[k]r^*[n+1,k] \tag{5.25}$$

Substituting (5.20) and (5.21) into (5.24) and (5.25):

$$\tilde{s}_1[n,k] = \left(\left| \hat{H}_1[k] \right|^2 + \left| \hat{H}_2[k] \right|^2 \right) s_1[n,k] + \hat{H}_1^*[k]w[n,k] + \hat{H}_2[k]w^*[n+1,k] \tag{5.26}$$

$$\tilde{s}_2[n,k] = \left(\left| \hat{H}_1[k] \right|^2 + \left| \hat{H}_2[k] \right|^2 \right) s_2[n,k] + \hat{H}_2^*[k]w[n,k] - \hat{H}_1[k]w^*[n+1,k] \tag{5.27}$$

Radar terminal

Consider a RadCom system with Q Rx antennas and two transmit antennas. At the Radar terminal, the signal receives the echoes from the objects in the field. Considering only the angle and the Doppler shift effects and $H = 1$ target, the channel correspondent to the Tx antennas 1, can be express as,

$$G_{1,q} = e^{j2\pi T_0 f_D l} \cdot e^{-2j\pi f_c \tau_q}. \tag{5.28}$$

Being the second Tx antenna spaced by a $Q \times \frac{\lambda}{2}$ distance from the first the channel relative to the second antenna, can be express as,

$$G_{2,q} = G_{1,q} \cdot e^{-j2\pi f_c Q \frac{\lambda}{2} \frac{\sin \Theta}{c_0}} \tag{5.29}$$

The received signal at the $q = 1$ index of the virtual array for a $l = 1$ index of the OFDM symbol, is given by

$$\begin{bmatrix} r[n,k] \\ r[n+1,k] \end{bmatrix} = \begin{bmatrix} s_1[n,k] & s_2[n,k] \\ s_1[n+1,k] & s_2[n+1,k] \end{bmatrix} \begin{bmatrix} G_1[k]_{1,l} \\ G_2[k]_{1,l} \end{bmatrix} + \begin{bmatrix} w_1 \\ w_2 \end{bmatrix} \tag{5.30}$$

In order to separate the symbols from the radar parameters, is implemented the following calculation to estimate the vector channel,

$$\begin{bmatrix} G_1[\hat{k}]_{1,l} \\ G_2[\hat{k}]_{1,l} \end{bmatrix} = \begin{bmatrix} s_1^*[n,k] & -s_1[n+1,k] \\ s_2^*[n,k] & s_2[n+1,k] \end{bmatrix} \begin{bmatrix} r[n,k] \\ r[n+1,k] \end{bmatrix} + \begin{bmatrix} w_1 \\ w_2 \end{bmatrix} \tag{5.31}$$

From the equation (5.31),

$$G_{l,q}[k] \approx [\hat{G}_{1,q,l} \ \hat{G}_{2,q,l}], \ \ k = 0, ..., N - 1. \tag{5.32}$$

The information from 5.32 is stored into the matrix $F_q(k,l)$ as

$$F_q(k,l) = G_{l,q}[k]. \tag{5.33}$$

The resulting matrix $F_q(k,l)$ has a dimension of $N \times M$. In order to calculate the radar parameters the process is the same as the one presented in section 5.2.2.

5.4 Performance Results

In this section, the performance of the OFDM MIMO Radar and the RadCom System proposed is evaluated. The waveform of the two systems operates at 24GHz ISM band with a bandwidth $B = 93.1$MHz. Being the bandwidth of the signal a fixed value and the range resolution dependent only on the bandwidth, the value of range resolution is $\Delta r = 1.61m$, for all the scenarios considered. The limiting properties of the channel are the Doppler spread and the maximum delay. The magnitude of every target reflection is not taken into account.

This section is divided in three parts, the first part presents the various scenarios for the OFDM SISO radar system, the second the MIMO radar system developed and the third part the RadCom system. We present various scenarios with different waveform parameters and different target parameters.

In this Section we present results for several scenarios: 1 up to 4 for OFDM single antenna Radar system, 5 and 6 for OFDM MIMO Radar System and 7 for RadCom System.

5.4.1 Imaging performance with OFDM Radar System developed

Consider Table 5.2 where the target parameters are defined for the scenarios studied in this section. Along with the target parameters, consider the following notation: (N, M, P, Q) to denote a system using N subcarriers, M symbols, P transmit antennas and Q receive antennas.

Table 5.2: Target parameters.

Target	Velocity	Range
A	5 m/s	2 m
B	5 m/s	0 m
C	0 m/s	10 m
D	10 m/s	20 m
E	9 m/s	19 m
F	0 m/s	40 m

In the scenario 1 and 2 we analyze for the Target A, how the waveform parameters affect the resolution of the target. Considering a $(256, 32, 1, 1)$ SISO Radar System for the scenario 1

along with the Radar specifications presented by table 5.3, and a $(1024, 256, 1, 1)$ SISO Radar System for the scenario 2, where table 5.4 give us the radar specifications for the scenario 2.

Table 5.3: Radar Specifications: Scenario 1.

Velocity Resolution Δv	$71.03 m/s$
Subcarriers spacing Δf	$363.7 kHz$
OFDM symbol duration T	$2.7\ \mu s$

Table 5.4: Radar Specifications: Scenario 2.

Velocity Resolution Δv	$2.22 m/s$
Subcarriers spacing Δf	$90.09 kHz$
OFDM symbol duration T	$11 \mu s$

Figure 5.5 shows the radar imaging for the scenario 1 and the radar imaging for the scenario 2.
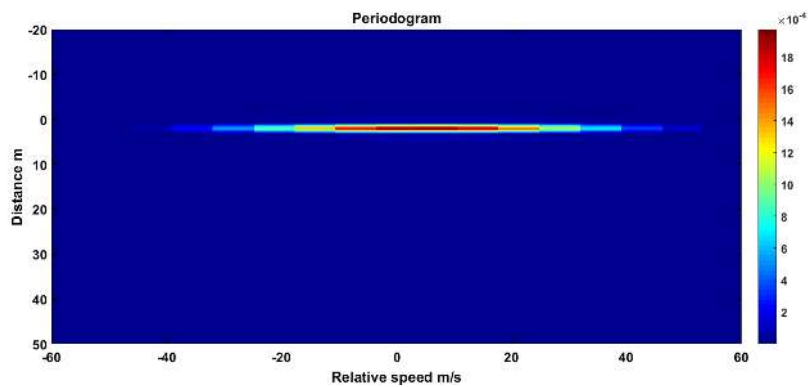
(a) Radar imaging for the Target A; and Radar Specifications: Scenario 1.
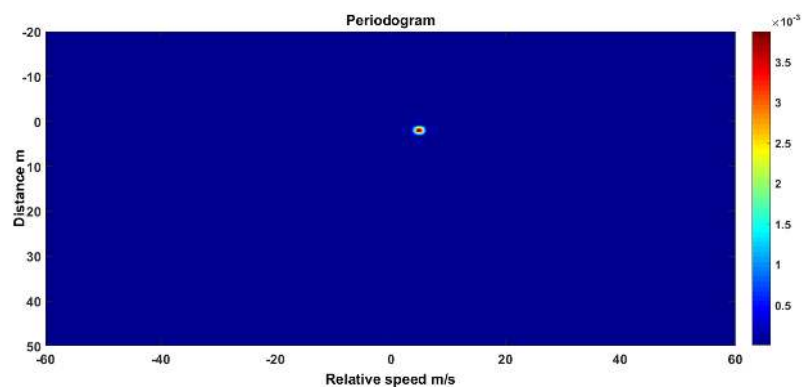
(b) Radar imaging for the Target A; and Radar Specifications: Scenario 2.

Figure 5.5: Scenario 1 and Scenario 2.

Analyzing the scenarios 1 and 2 as result of the simulations for the same target parameters and for different radar specifications, it is possible to see how the waveform parameters affect

the radar resolution. Considering the scenario 1 and 2 it is possible to obtain a good range resolution, but the simulation presents a coarse velocity resolution. Increasing the number of subcarriers and OFDM symbols the OFDM Radar system presents a considerable improvement in the resolution parameters as we can see from the simulation results presented for scenario 2, Figure 5.5b.

In next simulations, considering a (1024,256,1,1) SISO Radar System we present a radar imaging for several targets, with Radar Specifications given by Table 5.5.

Table 5.5: Radar Specifications: Scenarios 3,4.

Velocity Resolution Δv	$2.22m/s$
Subcarriers spacing Δf	$90.09kHz$
OFDM symbol duration T	$11\mu s$

In scenario 3 the targets B, C and D are considered and for the scenario 4 the targets D, E and F are considered. Figure 5.6 shows the radar imaging for the scenario 3 and the radar imaging for the scenario 4.
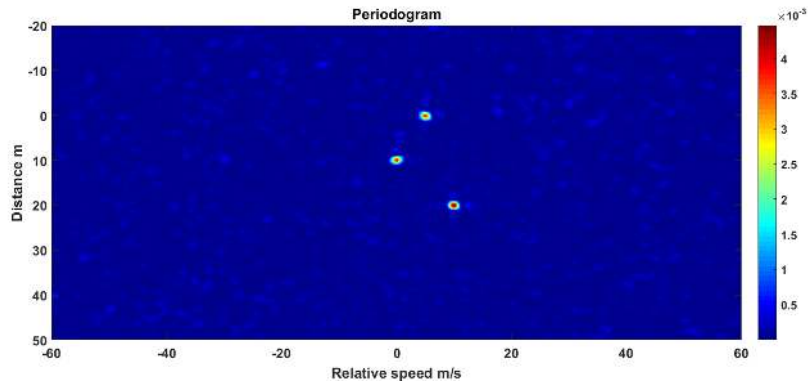
(a) Radar imaging for the Targets: B, C, D;and Radar Specifications: Scenario 3.
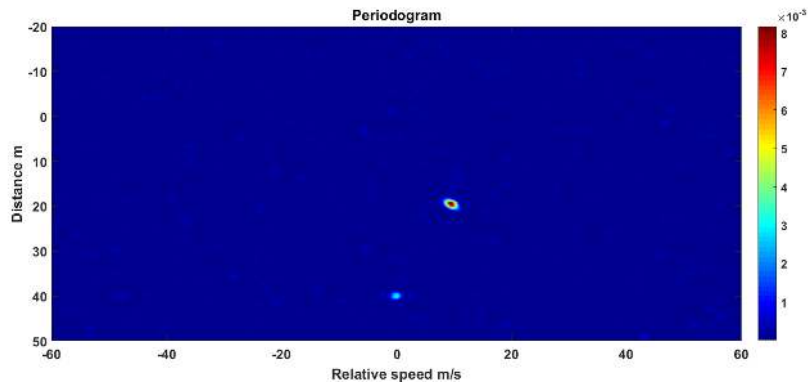
(b) Radar imaging for the Targets: D, E, F;and Radar Specifications: Scenario 4.

Figure 5.6: Scenario 3 and Scenario 4.

In the scenario 4 was simulated a periodogram for a case where the radar constraints are

not met. It is possible to conclude that the radar algorithm cannot distinguish the Target D and Target E because the distance between them is less than the resolution parameters.

5.4.2   Imaging performance with OFDM MIMO Radar System developed

In this section we present the simulations of a MIMO system studied in chapter 4, by simulating the equivalent virtual array concept. Table 5.6 give us the target parameters and Table 5.7 the Radar Specifications, studied in this section. Consider as well the $(1024, 256, 3, 5)$ MIMO Radar system.

Table 5.6: Target parameters.

Target	Angle	Range
A	$40°$	$50m$
B	$50°$	$100m$

Target	Angle	Velocity
C	$30°$	$100m/s$
D	$45°$	$80m/s$

Table 5.7: Radar Specifications: Scenarios 5, 6.

Velocity Resolution Δv	$2.22m/s$
Angle Resolution $\Delta\Theta$	$3.8°$
Subcarriers spacing Δf	$90.09kHz$
OFDM symbol duration T	$11\ \mu s$

Figure 5.7 shows the radar imaging for the scenario 5 and the radar imaging for the scenario 6.
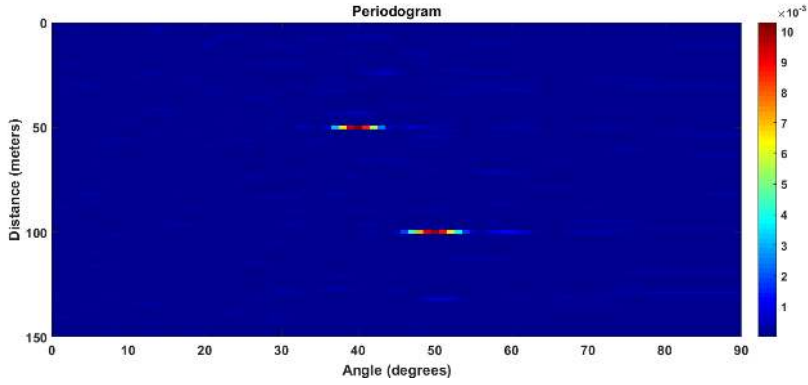
(a) Radar imaging for the Targets: A, B; and Radar Specifications: Scenario 5.
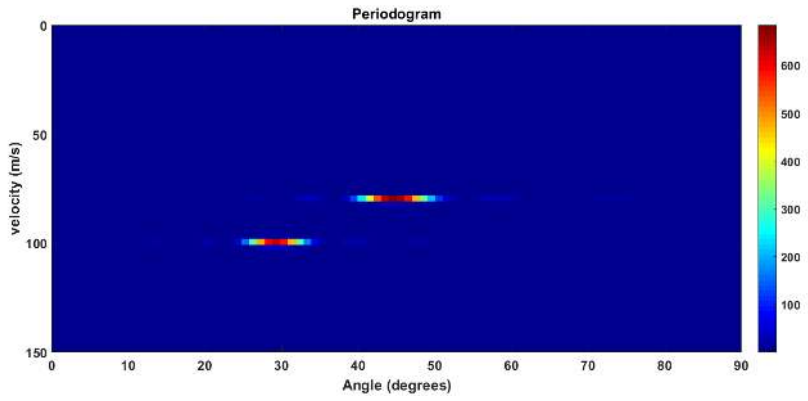
(b) Radar imaging for the Targets: C, D; and Radar Specifications: Scenario 6.

Figure 5.7: Scenario 5 and Scenario 6.

In scenario 5 was simulated a periodogram where the radar parameters are range and angle and it was considered the target A and B. In scenario 6 was simulated a periodogram where the radar parameters are velocity and angle and it was considered the target C and D. The radar has managed to solve the 4 targets, since the resolution parameters agree with the target parameters.

5.4.3 Imaging performance with RadCom System developed

For the scenario 7, we present the average BER performance over a predefined E_b/N_0 for the communication terminal designed in this section 5.3 and a radar imaging performed at the RadCom System designed. Consider the $(1024, 256, 2, 10)$ RadCom System. The target parameters are described in Table 5.8 and the radar specifications in Table 5.9.

Table 5.8: Target parameters.

Target	Angle	Velocity
A	30°	$100m/s$

Table 5.9: Radar Specifications: Scenarios 7.

Velocity Resolution Δv	$2.22m/s$
Angle Resolution $\Delta\Theta$	$3.8°$
Subcarriers spacing Δf	$90.09kHz$
OFDM symbol duration T	$11\ \mu s$

The Figure 5.8 shows the radar imaging performed from the RadCom system developed and the BER at the communication terminal.
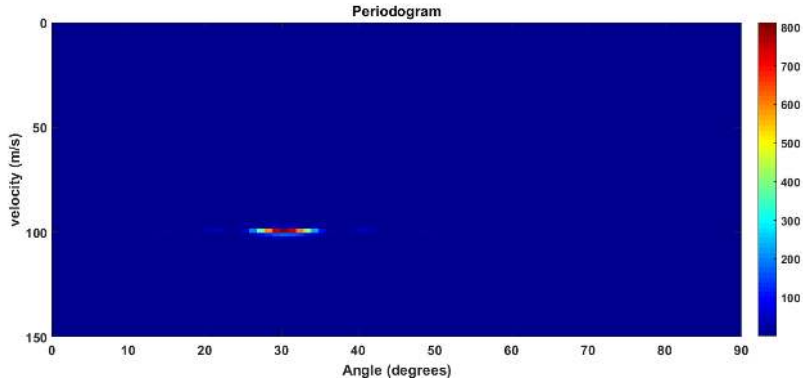
(a) Radar imaging for the Target: A;and Radar Specifications: Scenario 7.
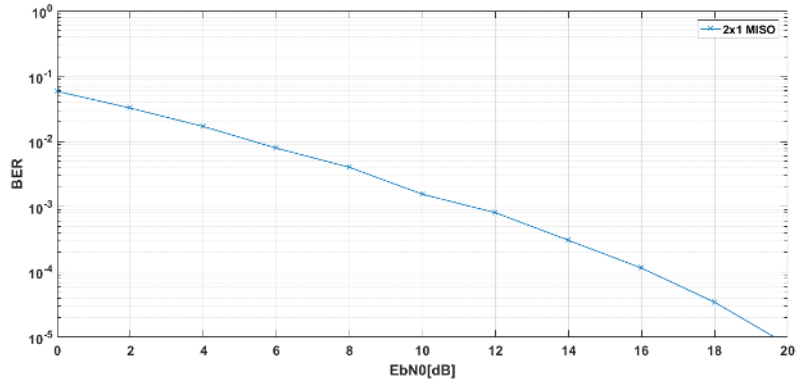
(b) BER perfomance at the Communication terminal.

Figure 5.8: Scenario 7 and BER.

It can be seen that the inclusion of the communication functionality in the MIMO Radar system, comprising the signal-sharing technique previously described to recover the payload data, was achieved successfully. Namely, a viable communication link between the RadCom system and the communication terminal was accopmlished and a way to integrate both radar and communication functionalities, within the RadCom system developed.

Chapter 6

Conclusions and Future Work

In this chapter, we present the conclusions of this work and a possible points for the future work.

6.1 Conclusions

In this dissertation we started by presenting the background of the communications system and the evolution since the first generation to the next generation. From the description presented in this chapter, we can see the progress made from the 1G until the current technology systems, the future communications systems are expected to provide very high data rates with a low latency. Consequently, we also face a spectrum congestion problem which leads the focus of research work in new applications with better use of the spectrum resources. Motivated by this needs emerged the idea to develop a system with integrated radar and communication technology in the same device. The chapter 1, presents an overview of the joint radar and communication system showing the advantages for future communications systems.

In chapter 2, the radar system and the basics of the system were introduced. It was presented the operational frequency band of the radar systems, the radar equation and the radar waveforms. It was also introduced such features of the radar in order to help the design of a radar system.

Then, in chapter 3 were introduced the OFDM radar system. We started by presenting an overview of the OFDM waveform and some communications requirements. Later, were presented the OFDM waveform as the signal model for radar systems. In the end of the chapter, it was presented the boundaries of the OFDM radar system. It was possible to conclude that OFDM fits the radar parameters as a choice for radar waveform.

In chapter 4, were presented the modifications of the OFDM system with the introduction of multiple antenna systems. We started by presenting an overview of systems that employ multiple antennas, at the transmitter and receiver, allowing to obtain diversity, spatial multiplexing and higher data rates. After, it was introduced the antenna configuration and presented the angle estimation basics. Furthermore, it was also described the MIMO Radar with OFDM as signal model.

In chapter 5, were proposed an OFDM MIMO radar system model without communication and the development of a radar imaging. Later, it was added communications in the radar system by combining the Alamouti code with OFDM for the integration of MIMO Radar and Communication Systems.

A joint radar and communication system has significant advantages in terms of cost, size, performance and spectrum usage. The integration of radar and communication systems is accomplished by using OFDM as a common waveform and the use of Alamouti coding enables both the achievement of spatial diversity, for the communication functionality, and of transmit signal orthogonality required to improve resolution, for the radar functionality. The flexible allocation of carriers was one of the motivation for choosing OFDM as a candidate radar signal. The evaluation made of such technologies to achieve radar and communication integration was accomplished by developing a simulation platform, first only with the radar functionality, for SISO and MIMO configurations, and then with both radar and communication functionalities. The evaluation results of this work took us to the following conclusion:

- The OFDM is a viable choice for radar and exhibits good values for the resolution parameter and for the radar performance.

- The performance of a radar imaging with the main target parameters such, range, velocity and angle were simulated with success through the systems studied and developed, in this work.

- The simulations showed that it is possible by means of a shared waveform preserve the information and maintain the radar functionality at same time, from a node RadCom system to a communication device.

6.2 Future Work

As possible points for future work the following topics may be considered among others:

- The demonstration of the MIMO OFDM Radar and Communication system in practical scenarios by implementing in hardware the techniques studied and evaluated in this work.

- This work considers a scenario with only one radar or RadCom terminal. An important aspect to be considered as future work would be the study of the impact incurred by the deployment of several terminals working using the same space-time-frequency resources. Namely, the analysis of the interference among RadCom terminals and the exploration of coexistence and interference removal techniques.

- OFDM is a well known waveform, especially for communication applications. However, other waveforms have been proposed and studied recently for commnication systems. Among them we have the Universal Filtered Multicarrier (UFMC), Generalized Frequency Division Multiplexing (GFDM) and Filter Bank Multicarrier (FBMC). Therefore, the study of these waveforms for RadCom would be also an important future work.

Bibliography

[1] MMUI Mir and S Kumar. Evolution of mobile wireless technology from og to 5g. *International Journal of Computer Science and Information Technologies*, 6(3):2545–2551, 2015.

[2] Pankaj Sharma. Evolution of mobile wireless communication networks-1g to 5g as well as future prospective of next generation communication network. *International Journal of Computer Science and Mobile Computing*, 2(8):47–53, 2013.

[3] A. Silva A. Gameiro. Comunicações sem fios (wireless communications). DETI, University of Aveiro, 2017.

[4] The evolution of mobile technologies:1g-2g-3g-4g lte. Available at `https://www.qualcomm.com/media/documents/files/download-the-evolution-of-mobile-technologies-1g-to-2g-to-3g-to-4g-lte-qualcomm.pdf`. Accessed on: 2018-10-10.

[5] Suk Yu Hui and Kai Hau Yeung. Challenges in the migration to 4g mobile systems. *IEEE Communications magazine*, 41(12):54–59, 2003.

[6] Arunabha Ghosh, Jun Zhang, Jeffrey G Andrews, and Rias Muhamed. *Fundamentals of LTE*. Pearson Education, 2010.

[7] Gary Boudreau, John Panicker, Ning Guo, Rui Chang, Neng Wang, and Sophie Vrzic. Interference coordination and cancellation for 4g networks. *IEEE Communications Magazine*, 47(4), 2009.

[8] Sven Mattisson. Overview of 5g requirements and future wireless networks. In *ESSCIRC 2017-43rd IEEE European Solid State Circuits Conference*, pages 1–6. IEEE, 2017.

[9] Qingqing Wu, Geoffrey Ye Li, Wen Chen, Derrick Wing Kwan Ng, and Robert Schober. An overview of sustainable green 5g networks. *IEEE Wireless Communications*, 24(4): 72–80, 2017.

[10] Jeffrey G Andrews, Stefano Buzzi, Wan Choi, Stephen V Hanly, Angel Lozano, Anthony CK Soong, and Jianzhong Charlie Zhang. What will 5g be? *IEEE Journal on selected areas in communications*, 32(6):1065–1082, 2014.

[11] V2x solutions for autonomous vehicle: 5g or ieee 802.11p? Available at `https://movimentogroup.com/blog/v2x-solutions-autonomous-vehicle-5g-ieee-802-11p/`. Accessed on: 2018-10-08.

[12] Recommendations on 5g requirements and solutions. Available at `http://www.5gamericas.org/files/2714/1471/2645/4G_Americas_Recommendations_on_5G_Requirements_and_Solutions_10_14_2014-FINALx.pdf`. Accessed on: 2018-10-20.

[13] Guangyi Liu and Dajie Jiang. 5g: Vision and requirements for mobile communication system towards year 2020. *Chinese Journal of Engineering*, 2016, 2016.

[14] Faisal Alsubaei, Abdullah Abuhussein, and Sajjan Shiva. An overview of enabling technologies for the internet of things. *Internet of Things A to Z: Technologies and Applications*, pages 77–112, 2018.

[15] Luigi Atzori, Antonio Iera, and Giacomo Morabito. The internet of things: A survey. *Computer networks*, 54(15):2787–2805, 2010.

[16] Werner Wiesbeck and Leen Sit. Radar 2020: The future of radar systems. In *Radar Conference (Radar), 2014 International*, pages 1–6. IEEE, 2014.

[17] Werner Wiesbeck. The radar of the future. In *Radar Conference (EuRAD), 2013 European*, pages 137–140. IEEE, 2013.

[18] Stanisław Rzewuski and Krzysztof Kulpa. System concept of wifi based passive radar. *International Journal of Electronics and Telecommunications*, 57(4):447–450, 2011.

[19] Dale Gould, Robert Pollard, Carlos Sarno, and Paul Tittensor. A multiband passive radar demonstrator. In *Radar Symposium, 2006. IRS 2006. International*, pages 1–4. IEEE, 2006.

[20] Marcin K Baczyk, Piotr Samczynski, Piotr Krysik, and Krzysztof Kulpa. Traffic density monitoring using passive radars. *IEEE Aerospace and Electronic Systems Magazine*, 32(2):14–21, 2017.

[21] Andrey Garnaev, Wade Trappe, and Athina Petropulu. Bargaining over fair performing dual radar and communication task. In *Signals, Systems and Computers, 2016 50th Asilomar Conference on*, pages 47–51. IEEE, 2016.

[22] Christian Sturm, Thomas Zwick, and Werner Wiesbeck. An ofdm system concept for joint radar and communications operations. In *Vehicular Technology Conference, 2009. VTC Spring 2009. IEEE 69th*, pages 1–5. IEEE, 2009.

[23] Kiyoshi Mizui, Masatoshi Uchida, and Masao Nakagawa. Vehicle-to-vehicle communication and ranging system using spread spectrum technique (proposal of boomerang transmission system). In *Vehicular Technology Conference, 1993., 43rd IEEE*, pages 335–338. IEEE, 1993.

[24] R Cager, D LaFlame, and L Parode. Orbiter ku-band integrated radar and communications subsystem. *IEEE Transactions on Communications*, 26(11):1604–1619, 1978.

[25] Shannon D Blunt, Matthew R Cook, and James Stiles. Embedding information into radar emissions via waveform implementation. In *Waveform Diversity and Design Conference (WDD), 2010 International*, pages 000195–000199. IEEE, 2010.

[26] Aboulnasr Hassanien, Moeness G Amin, Yimin D Zhang, and Fauzia Ahmad. Signaling strategies for dual-function radar communications: an overview. *IEEE Aerospace and Electronic Systems Magazine*, 31(10):36–45, 2016.

[27] Nadav Levanon. Multifrequency radar signals. In *Radar Conference, 2000. The Record of the IEEE 2000 International*, pages 683–688. IEEE, 2000.

[28] GEA Franken, H Nikookar, and Piet Van Genderen. Doppler tolerance of ofdm-coded radar signals. In *Radar Conference, 2006. EuRAD 2006. 3rd European*, pages 108–111. IEEE, 2006.

[29] BJ Donnet and ID Longstaff. Combining mimo radar with ofdm communications. In *Radar Conference, 2006. EuRAD 2006. 3rd European*, pages 37–40. IEEE, 2006.

[30] Chowdhury Shahriar, Ahmed Abdelhadi, and T Charles Clancy. Overlapped-mimo radar waveform design for coexistence with communication systems. In *Wireless Communications and Networking Conference (WCNC), 2015 IEEE*, pages 223–228. IEEE, 2015.

[31] Christian Sturm and Werner Wiesbeck. Waveform design and signal processing aspects for fusion of wireless communications and radar sensing. *Proceedings of the IEEE*, 99(7): 1236–1259, 2011.

[32] Liang Han and Ke Wu. Joint wireless communication and radar sensing systems–state of the art and future prospects. *IET Microwaves, Antennas & Propagation*, 7(11):876–885, 2013.

[33] Holger H Meinel. Evolving automotive radar—from the very beginnings into the future. In *Antennas and Propagation (EuCAP), 2014 8th European Conference on*, pages 3107–3114. IEEE, 2014.

[34] Bryan Paul, Alex R Chiriyath, and Daniel W Bliss. Survey of rf communications and sensing convergence research. *IEEE Access*, 5:252–270, 2017.

[35] Panos Papadimitratos, Arnaud De La Fortelle, Knut Evenssen, Roberto Brignolo, and Stefano Cosenza. Vehicular communication systems: Enabling technologies, applications, and future outlook on intelligent transportation. *IEEE communications magazine*, 47 (11), 2009.

[36] Tesla motors. Available at `https://www.tesla.com/pt_PT/models`. Accessed on: 2018-10-14.

[37] ETSI (European Telecommunications Standards Institute). Intelligent transport systems. Available at `http://www.esa.int/spaceinimages/Images/2017/09/People_mobility`. Accessed on: 2018-10-08.

[38] Preeti Kumari, Nuria Gonzalez-Prelcic, and Robert W Heath. Investigating the ieee 802.11 ad standard for millimeter wave automotive radar. In *Vehicular Technology Conference (VTC Fall), 2015 IEEE 82nd*, pages 1–5. IEEE, 2015.

[39] Joseph B. Evans. Shared spectrum access for radar and communications (ssparc). Available at `https://www.darpa.mil/program/`

`shared-spectrum-access-for-radar-and-communications`. Accessed on: 2018-10-10.

[40] Zaheer Khan, Janne J Lehtomaki, Stefano Iellamo Iellamo, Risto Vuohtoniemi, Ekram Hossain, and Zhu Han. Iot connectivity in radar bands: A shared access model based on spectrum measurements. *IEEE Communications Magazine*, 55(2):88–96, 2017.

[41] Christian Sturm, Yoke Leen Sit, Martin Braun, and Thomas Zwick. Spectrally interleaved multi-carrier signals for radar network applications and multi-input multi-output radar. *IET Radar, Sonar & Navigation*, 7(3):261–269, 2013.

[42] Anil K Maini. *Handbook of Defence Electronics and Optronics: Fundamentals, Technologies and Systems*. John Wiley & Sons, 2018.

[43] Haleema Sadia, Sabahat Sherien, Hafsa Iqbal, Muhammad Zeeshan, Aimal Khan, and Saad Rehman. Range estimation in radar using maximum likelihood estimator. In *Computer and Information Technology (ICCIT), 2017 20th International Conference of*, pages 1–5. IEEE, 2017.

[44] Christian Wolff. Radar basics. Available at `http://www.radartutorial.eu/01.basics/Range%20Resolution.en.html`. Accessed on: 2018-09-28.

[45] Ann ML Cavallo, Wendell H Potter, and Michelle Rozman. Gender differences in learning constructs, shifts in learning constructs, and their relationship to course achievement in a structured inquiry, yearlong college physics course for life science majors. *School Science and Mathematics*, 104(6):288–300, 2004.

[46] JA Bruder, JT Carlo, JH Gurney, and J Gorman. Ieee standard for letter designations for radar-frequency bands. *IEEE Aerospace & Electronic Systems Society*, pages 1–3, 2003.

[47] Niraj Prasad Bhatta and M GeethaPriya. Radar and its applications.

[48] Merrill I Skolnik. Introduction to radar. *Radar handbook*, 2, 1962.

[49] Mark A Richards. *Fundamentals of radar signal processing*. Tata McGraw-Hill Education, 2005.

[50] Sujeet Milind Patole, Murat Torlak, Dan Wang, and Murtaza Ali. Automotive radars: A review of signal processing techniques. *IEEE Signal Processing Magazine*, 34(2):22–35, 2017.

[51] CJ Baker and HD Griffiths. Radar systems and waveforms. In *Waveform Diversity & Design Conference, 2004. WDD2004 2004. International*, pages 1–7. IEEE, 2004.

[52] Mark A Richards, Jim Scheer, William A Holm, and William L Melvin. *Principles of modern radar*. Citeseer, 2010.

[53] Yongjun Liu, Guisheng Liao, and Zhiwei Yang. Range and angle estimation for mimo-ofdm integrated radar and communication systems. In *Radar (RADAR), 2016 CIE International Conference on*, pages 1–4. IEEE, 2016.

[54] Yoke Leen Sit, Lars Reichardt, Christian Sturm, and Thomas Zwick. Extension of the ofdm joint radar-communication system for a multipath, multiuser scenario. In *Radar Conference (RADAR), 2011 IEEE*, pages 718–723. IEEE, 2011.

[55] Lang Hu, Zicheng Du, and Guangran Xue. Radar-communication integration based on ofdm signal. In *Signal Processing, Communications and Computing (ICSPCC), 2014 IEEE International Conference on*, pages 442–445. IEEE, 2014.

[56] Nadav Levanon. Radar principles. *New York, Wiley-Interscience, 1988, 320 p.*, 1988.

[57] Richard van Nee and Ramjee Prasad. *OFDM for wireless multimedia communications*. Artech House, Inc., 2000.

[58] William Y Zou and Yiyan Wu. Cofdm: An overview. *IEEE transactions on broadcasting*, 41(1):1–8, 1995.

[59] S Weinstein and Paul Ebert. Data transmission by frequency-division multiplexing using the discrete fourier transform. *IEEE transactions on Communication Technology*, 19(5): 628–634, 1971.

[60] Behrouz Farhang-Boroujeny. Ofdm versus filter bank multicarrier. *IEEE signal processing magazine*, 28(3):92–112, 2011.

[61] Lajos Hanzo, Soon Xin Ng, WT Webb, and T Keller. *Quadrature amplitude modulation: From basics to adaptive trellis-coded, turbo-equalised and space-time coded OFDM, CDMA and MC-CDMA systems*. IEEE Press-John Wiley, 2004.

[62] Emad Hassan. *Multi-carrier communication systems with examples in MATLAB®: A new perspective*. CRC Press, 2016.

[63] Concepts of orthogonal frequency division multiplexing (ofdm) and 802.11 wlan. Available at `http://rfmw.em.keysight.com/wireless/helpfiles/89600b/webhelp/subsystems/wlan-ofdm/content/ofdm_basicprinciplesoverview.htm`. Accessed on: 2018-09-30.

[64] Dipl-Ing Martin Braun. Ofdm radar algorithms in mobile communication networks. 2014.

[65] Martin Braun, Christian Sturm, Andreas Niethammer, and Friedrich K Jondral. Parametrization of joint ofdm-based radar and communication systems for vehicular applications. In *Personal, Indoor and Mobile Radio Communications, 2009 IEEE 20th International Symposium on*, pages 3020–3024. IEEE, 2009.

[66] Kh Tovmasyan. Ofdm signal constellation processing on radar applications. *Armenian Journal of Physics*, 6(4):204–208, 2013.

[67] Yoke Leen Sit, Christian Sturm, and Thomas Zwick. Doppler estimation in an ofdm joint radar and communication system. In *Microwave Conference (GeMIC), 2011 German*, pages 1–4. IEEE, 2011.

[68] Christian Sturm, Elena Pancera, Thomas Zwick, and Werner Wiesbeck. A novel approach to ofdm radar processing. In *Radar Conference, 2009 IEEE*, pages 1–4. IEEE, 2009.

[69] Martin Braun, Yves Koch, Christian Sturm, and Friedrich K Jondral. Signal design and coding for high-bandwidth ofdm in car-to-car communications. In *Vehicular Technology Conference Fall (VTC 2010-Fall), 2010 IEEE 72nd*, pages 1–5. IEEE, 2010.

[70] Alexander Ganis, Enric Miralles, Christoph Heller, Ulrich Prechtel, Askold Meusling, Heinz-Peter Feldle, Mirko Loghi, Frank Ellinger, and Volker Ziegler. A system concept for a 3d real-time ofdm mimo radar for flying platforms. In *Microwave Conference (GeMiC), 2016 German*, pages 201–204. IEEE, 2016.

[71] Yoke Leen Sit and Thomas Zwick. Mimo ofdm radar with communication and interference cancellation features. In *Radar Conference, 2014 IEEE*, pages 0265–0268. IEEE, 2014.

[72] Harri Holma and Antti Toskala. *LTE for UMTS: OFDMA and SC-FDMA based radio access*. John Wiley & Sons, 2009.

[73] Jorge Garcia-Fragoso and Giselle M Galvan-Tejada. Cell planning based on the wimax standard for home access: A practical case. In *Electrical and Electronics Engineering, 2005 2nd International Conference on*, pages 89–92. IEEE, 2005.

[74] Jeffrey G Andrews, Arunabha Ghosh, and Rias Muhamed. *Fundamentals of WiMAX: understanding broadband wireless networking*. Pearson Education, 2007.

[75] Gerard J Foschini. Layered space-time architecture for wireless communication in a fading environment when using multi-element antennas. *Bell labs technical journal*, 1(2): 41–59, 1996.

[76] Eran Fishler, Alexander Haimovich, Rick S Blum, Leonard J Cimini, Dmitry Chizhik, and Reinaldo A Valenzuela. Spatial diversity in radars—models and detection performance. *IEEE Transactions on Signal Processing*, 54(3):823–838, 2006.

[77] Jerry R Hampton. *Introduction to MIMO communications*. Cambridge university press, 2013.

[78] Mimo formats - siso, simo, miso, mu-mimo. Available at `https://www.electronics-notes.com/articles/antennas-propagation/mimo/siso-simo-miso-mimo.php`. Accessed on: 2018-10-08.

[79] Yibo Jiang, Haitong Sun, Sharad Sambhwani, and Jilei Hou. Uplink closed loop transmit diversity for hspa. *Qualcomm Incorporated, May*, 19, 2010.

[80] Siavash M Alamouti. A simple transmit diversity technique for wireless communications. *IEEE Journal on selected areas in communications*, 16(8):1451–1458, 1998.

[81] Alexander M Haimovich, Rick S Blum, and Leonard J Cimini. Mimo radar with widely separated antennas. *IEEE Signal Processing Magazine*, 25(1):116–129, 2008.

[82] Ying Liu and Hongyuan Cui. Antenna array signal direction of arrival estimation on digital signal processor (dsp). *Procedia Computer Science*, 55:782–791, 2015.

[83] Yoke Leen Sit, Thuy T Nguyen, Christian Sturm, and Thomas Zwick. 2d radar imaging with velocity estimation using a mimo ofdm-based radar for automotive applications. In *Radar Conference (EuRAD), 2013 European*, pages 145–148. IEEE, 2013.

[84] KW Forsythe, DW Bliss, and GS Fawcett. Multiple-input multiple-output (mimo) radar: Performance issues. In *Signals, Systems and Computers, 2004. Conference Record of the Thirty-Eighth Asilomar Conference on*, volume 1, pages 310–315. IEEE, 2004.

[85] Thanh Thuy Nguyen. Design and analysis of superresolution algorithm and signal separation technique for an ofdm-based mimo radar. Master's thesis, Universitat Politècnica de Catalunya, 2012.

[86] Benjamin Nuss, Leen Sit, Michael Fennel, Jonathan Mayer, Tobias Mahler, and Thomas Zwick. Mimo ofdm radar system for drone detection. In *Radar Symposium (IRS), 2017 18th International*, pages 1–9. IEEE, 2017.

[87] HT Hayvaci and B Tavli. Spectrum sharing in radar and wireless communication systems: A review. In *Electromagnetics in Advanced Applications (ICEAA), 2014 International Conference on*, pages 810–813. IEEE, 2014.

[88] Yu Zhang, Qingyu Li, Ling Huang, and Jian Song. Waveform design for joint radar-communication system with multi-user based on mimo radar. In *Radar Conference (RadarConf), 2017 IEEE*, pages 0415–0418. IEEE, 2017.

[89] Martin Braun, Christian Sturm, and Friedrich K Jondral. Maximum likelihood speed and distance estimation for ofdm radar. In *Radar Conference, 2010 IEEE*, pages 256–261. IEEE, 2010.

[90] Eran Fishler, Alex Haimovich, Rick Blum, Dmitry Chizhik, Len Cimini, and Reinaldo Valenzuela. Mimo radar: An idea whose time has come. In *Radar Conference, 2004. Proceedings of the IEEE*, pages 71–78. IEEE, 2004.

[91] Cong Li, Weimin Bao, Luping Xu, Hua Zhang, and Ziyang Huang. Radar communication integrated waveform design based on ofdm and circular shift sequence. *Mathematical Problems in Engineering*, 2017, 2017.

[92] Yufei W Blankenship, Philippe J Sartori, Brian K Classon, Vip Desai, and Kevin L Baum. Link error prediction methods for multicarrier systems. In *Vehicular Technology Conference, 2004. VTC2004-Fall. 2004 IEEE 60th*, volume 6, pages 4175–4179. IEEE, 2004.

[93] Ashu Taneja, Surbhi Sharma, and Rajesh Khanna. Real-time channel estimation for ofdm system with alamouti-based stbc on test bed.